Deep–Sea Research II 218 (2024) 105433

Contents lists available at ScienceDirect

Deep-Sea Research Part II

journal homepage: www.elsevier.com/locate/dsr2

Siliceous microfossil assemblages in the southern Emperor Seamount Chain sediments and their biogeographical and paleoceanographical implications

Lidiya N. Vasilenko [a,*], Ira B. Tsoy [a], Tatyana N. Dautova [b]

[a] V. I. Il'ichev Pacific Oceanological Institute, Far Eastern Branch, Russian Academy of Sciences, Vladivostok, 690041, Russian Federation
[b] A.V. Zhirmunsky National Scientific Center of Marine Biology, Far Eastern Branch, Russian Academy of Sciences, Vladivostok, 690041, Russian Federation

ARTICLE INFO

Handling Editor: Dr W Smith

Keywords:
Siliceous microplankton
Radiolarians
Diatoms
Silicoflagellates
Emperor seamount chain
Sediments

ABSTRACT

The taxonomic composition and abundance of siliceous microfossils in sediments is a valuable source of information about environmental changes at the sea surface today and in the geological past. This paper presents the results of a study of siliceous microplankton (radiolaria, diatoms, and silicoflagellates) in the surface calcareous sediments (silty foraminiferal oozes and sands) of the Nintoku, Jingu, Ojin, Koko, and Yuryaku guyots at the southern end of the Emperor Seamount Chain (ESC). Bottom sediments were collected using an underwater remote-operated vehicle (ROV) Comanche-18. The study revealed the taxonomic diversity and relatively high abundance of siliceous microplankton. Radiolarians are represented by 237 taxa (104 taxa from 68 genera of Spumellaria, 120 taxa from 61 genera of Nassellaria, and 13 taxa from 7 genera of Collodaria). Diatoms are represented by 60 species from 29 genera, and silicoflagellates by 5 species from 3 genera. Differences in siliceous microplankton reflect the northern boundary of warm water in the ESC, passing at approximately 38°N, between the Jingu and Ojin guyots, which coincides with the boundary of the Kuroshio Bifurcation Current, confirmed by the corals and the bathyal fauna of brittle stars (*Ophiura*). The absence of remains of siliceous microplankton in some sediments is probably due to dissolution, and the presence of extinct taxa from older sedimentary rocks and neritic species is due to process of reworking caused by active hydrodynamics on ESC guyots and transport by currents.

1. Introduction

Radiolarians, diatoms, and silicoflagellates, whose skeletons and frustules are composed of biogenic silica, play an important role in the cycling of silicon and carbon in the oceans and revealing changes in the past and present (Nelson et al., 1995; Wong et al., 1995; Harrison, 2000; Zhang et al., 2015; Tréguer et al., 2018). The siliceous skeletons of radiolarians and silicoflagellates, as well as the diatom frustules, are well preserved in sediments after cell death and participate in various post-sedimentary processes, including the accumulation of siliceous sediments (Lisitsyn, 1974, 1978). Since these organisms are predominantly planktonic, their qualitative and quantitative distribution, both in the water column and after burial in sediments, is an indicator of certain physicochemical parameters of the environment (temperature, salinity) in which they lived (Dutkiewicz et al., 2016) as well as hydrodynamic processes affecting their transport, dissolution and burial. Changes in environmental parameters are reflected in the taxonomic composition and quantitative characteristics of siliceous microplankton (e.g. Harrison, 2000; Zhang et al., 2015; Tréguer et al., 2018), which is important for monitoring modern conditions, paleoreconstructions, and for models of changes in the natural environment in future.

Radiolarians are exclusively marine planktonic unicellular microorganisms that live at different depths, with salinity, as a rule, not lower than 31–32 (Kruglikova, 2013). Siliceous sediments and radiolarian oozes are composed of massive accumulations of radiolarian skeletons, which give them the status of rock-forming organisms. Their high abundance and rapid speciation allow them to be widely used in biostratigraphy. In addition, radiolarians are stenohaline organisms; they are highly sensitive to changes in salinity and water temperature (Tochilina, 1985; Afanasieva and Amon, 2006). Due to this, radiolarians are a good tool for establishing the stages of marine sedimentation in the geological past and in paleoclimatic reconstructions.

Diatoms and silicoflagellates are unicellular photosynthetic microalgae and are the first link in marine food webs. Silicoflagellates are exclusively marine, while diatoms account for a significant portion of the world's ocean productivity (e.g. Wong et al., 1995; Tréguer et al.,

---

[*] Corresponding author.
E-mail address: lidia@poi.dvo.ru (L.N. Vasilenko).

https://doi.org/10.1016/j.dsr2.2024.105433
Received 5 February 2024; Received in revised form 24 September 2024; Accepted 21 October 2024

2018). The distribution of diatoms and silicoflagellates in surface sediments reflects modern hydrological conditions (Sancetta and Silvestri, 1986; Kazarina and Yushina, 1999; Tsoy et al., 2009; Ren et al., 2014), which allows them to be used to reconstruct past environmental conditions.

The study area is located in the southern part of the Emperor Seamount Chain (ESC) (Fig. 1). A special feature of this area is its location in the transition zone of mixing water masses of the arctic-boreal and tropical zones. Comprehensive biostratigraphic studies of the sediments composing the ESC were carried out on during Deep Sea Drilling Project (DSDP) Legs 32 and 55, but radiolarians in these geological materials have not been extensively studied (Ling, 1980a). The Ojin (DSDP Site 430) and Nintoku (DSDP Site 432) guyots contain modern radiolarians, which are represented by species characteristic of the mid-latitude region of the North Pacific Ocean (Ling, 1980a). The taxonomic composition of the radiolarian community is unclear. The Yeoman Guyot (DSDP Site 431) yielded rare radiolarians from the Middle Pleistocene and is called the *Stylatractus universus* radiolarian Zone (also without taxonomic composition) (Ling, 1980a). During the Ocean Drilling Program (ODP) Sites 1205 and 1206 were drilled on the Nintoku and Koko guyots (Tarduno et al., 2002). Unfortunately, radiolarians were not studied in these.

Despite the limited study of radiolarians on the guyots of the ESC, there are numerous reports on the distribution and ecology of radiolarian species in the Pacific Ocean (Reshetnyak, 1966; Nigrini, 1970; Lombari and Boden, 1985; Yamauchi, 1986; Takahashi, 1991; Okazaki et al., 2004; Boltovskoy and Correa, 2016; Zhang et al., 2018). Near the ESC area, the radiolarian species diversity and abundance were studed in surface sediments along a 175°E transect from north to south (Motoyama and Nishimura, 2005; Kamikuri et al., 2008). Radiolarian assemblages from different climatic zones were traced using cluster analysis. In most modern studies, the boreal climatic zone is part of the subarctic zone and is rarely distinguished as an independent zone, as was done earlier (Lisitsyn, 1974; Ermakov et al., 1988). In addition, significant information was obtained on the depths and temperatures of some species of radiolarians, which also contributed to paleoceanographic reconstructions in the northern and central Pacific (Renz, 1976; Kling and Boltovskoy, 1995; Yamashita et al., 2002; Okazaki et al., 2005; Matsuzaki and Itaki, 2017; Matsuzaki et al., 2020).

Diatoms in the northwestern Pacific Ocean were studied in surface sediments (Belyaeva, 1963; Jousé et al., 1969; Sancetta and Silvestri, 1986; Tsoy and Wong, 1999; Kazarina and Yushina, 1999; Tsoy et al., 2009; Ren et al., 2014) and in plankton (Semina, 1974). In guyot sediments recovered by deep-sea drilling, diatoms of the Pleistocene-Holocene *Denticulopsis seminae* diatom Zone (Nintoku Guoyt) and *Pseudoeunotia doliolus* diatom Zone (Ojin and Koko guoyts) (Koizumi, 1980; Bukry, 1975), and modern silicoflagellates (Ojin and Nintoku guyots) (Ling, 1980b) were found.

The northwestern Pacific Ocean is characterized by two of the largest water structures – subarctic and subtropical, separated from each other by the Subarctic boundary (Dodimead et al., 1963). The subarctic boundary, located along 40°N, is formed by the intersection of the warm Kuroshio Current and the cold Oyashio Current (Chen et al., 2023) and separates colder, fresher water in the north from warmer, saltier water in the south (Yuan and Talley, 1996). The subarctic front is directed to the northeast and corresponds to the continuation of the cold Oyashio Current (Itoh et al., 2010). The warm Kuroshio Current flows northeast ward along the coast of Japan, then turns east at about 36°N, to become the Kuroshio Extension (KE) (Mizuno and White, 1983) (Fig. 1). The KE flows eastward at 37°N and 145°E, and the width of the fluctuating amplitude of the KE is termed the "Meander Zone" (Kawai, 1972; Motoyama and Nishimura, 2005). The KE usually bifurcates between 150° and 165°E (Mizuno and White, 1983). The Northern Branch (NB) of the KE, termed the Kuroshio Bifurcation Current, represents the northern boundary of the warm water carried by the Subtropical Gyre, flows east along 40°N, associated with the Kuroshio Bifurcation Front (Kawai, 1972; Mizuno and White, 1983). The Kuroshio Bifurcation Front is identified between 38° and 41°N (Roden et al., 1982; Zhang and Hanawa, 1993; Sainz-Trapaga et al., 2001). To the east of the "Meander Zone," the Kuroshio Current weakens, which is linked to the bathymetry encountered while flowing to the east, the Shatsky Rise and the ESC (Bernstein and White, 1981; Mizuno and White, 1983; Sainz-Trapaga

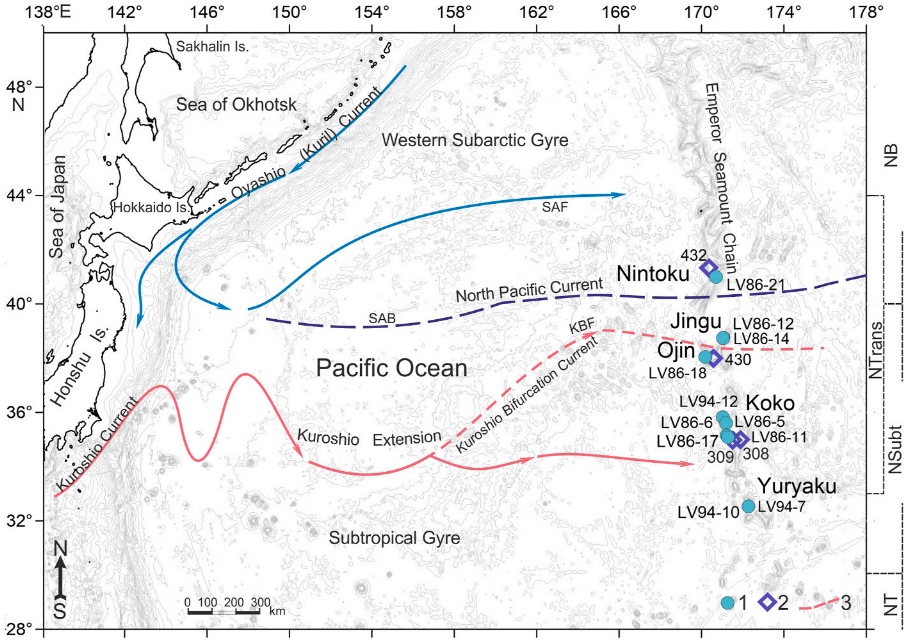

Fig. 1. A map of the studied sites on the ESC guyots and the scheme of major surface currents (Itoh and Yasuda, 2010; Chen et al., 2023). EKC – East Kamchatka Current, OYC – Oyashio Current, KC – Kuroshio Current, KE – Kuroshio Extension, KBF – Kuroshio Bifurcation Front, SAF – Subarctic Front, SAB – Subarctic Boundary. Climatic zones of North Pacific (Lisitsyn, 1974; Ermakov et al., 1988): NB – Boreal zone, NTrans - Transition zone, NSubt - Subtropical zone, NT- Tropical zone (boundary of NTrans by Kamikuri et al., 2008). 1 – studied sites, 2 – DSDP and ODP sites mentioned in this paper, 3 – the trajectory of the Kuroshio Bifurcation Current assumed in this study.

et al., 2001).

The ESC, which is an underwater ridge, stretches in the meridional direction for 2600 km from the coast of the Kamchatka Peninsula in the north (Meiji Guyot) to the northwestern end of the Hawaiian Ridge in the south. The ESC consists of seamounts 2–5 km high, some of which are flat-topped guyots (Davies et al., 1972; Karpoff et al., 1980; Clague and Dalrymple, 1987; Volokhin et al., 1995). They are united into linearly elongated massifs 450–600 km long and up to 150 km wide, separated by deep (5500–6000 m) sections (Vasiliev, 2009). The minimum depths of the mountain peaks are from 90 to 1245 m.

During DSDP Legs 32 and 55, and ODP Leg 197 several sites at Ojin, Yeomen, Nintoku, and Koko guyots were drilled (Clague and Dalrymple, 1973; Clague et al., 1975; Saito and Ozima, 1977; Dalrymple and Garcia, 1980; Jackson et al., 1980; Tarduno et al., 2002) and sediments of various lithology and ages were recovered (Karpoff, 1980; Karpoff et al., 1980; Koizumi et al., 1980; Tarduno et al., 2002). On the Nintoku, Yeomen, Ojin and Koko guyots, Paleocene and Eocene deposits are common, represented by calcareous and volcanic sandstones, sands with basalt pebbles, and pebbles. Upper Oligocene deposits recovered on the Koko Guyot and are represented by sandstones. Miocene and Pliocene deposits were found on the Yeomen and Nintoku guyots and are composed of diatomites, diatom-radiolaria and nanofossil siliceous oozes. Quaternary sediments on the Nintoku and Yeomen guyots are composed of sands with pebbles and gravels, clays, and calcareous sandstones. Yuryaku Guyot belongs to the Milwaukee Mountains series, the sediments of which are coral limestones and sedimentary rocks with shallow Neogene fauna (Clague et al., 1975). The ESC guyots consist of a volcanic basement and an overlying sedimentary cover, the lower part of which is represented predominantly by carbonate rocks formed in shallow water, and the upper part by deep-sea pelagic or hemipelagic silts (Volokhin et al., 1995). In the ESC, a decrease in the thickness of the sedimentary cover and the age of basal sediments is observed from north to south.

In the open subarctic Pacific Ocean, there are mainly two types of terrestrial sediments: aeolian dust (up to 90%) and clastic sediments transported by ocean currents (Wang et al., 2016). Chen et al. (2021) showed that the surface sediments of the ESC (~33°–44°N) are dominated by clayey silts, and at 1000–2500 m the average grain size of the silty sediments indicates active hydrodynamic conditions in the area.

The aim of the study is to identify the distribution features of siliceous microplankton – radiolarians, diatoms, and silicoflagellates in the surface calcareous sediments of the southern ESC guyots, in the transition zone from the arctic-boreal to the tropical region. These data are important for assessing the biodiversity of siliceous plankton in this zone and the likely migration of this zone at present and in the geological past.

2. Material and methods

2.1. Materials

Sediments were collected on the Nintoku, Jingu, Ojin, Koko, and Yuryaku guyots in the southern part of the ESC (Fig. 1) by the A.V. Zhirmunsky National Scientific Center of Marine Biology (NSCMB) together with the P.P. Shirshov Institute of Oceanology of the Russian Academy of Sciences during expeditions on the 86th and 94th cruises of the *R/V Akademik M.A. Lavrentyev* 2019, 2021. The bottom surface in most of the studied areas was an alternation of sedimentary and rock facies. Loose sediments are formed by eroded calcareous sand interspersed with small fragments of sedimentary and volcanic rocks (Dautova et al., 2019). The hard substrate is represented by tuffs, tuffaceous sandstones, limestones, as well as pillow and cover lavas of varying degrees of fragmentation, covered with a ferromanganese crust. A remotely operated underwater vehicle (ROV) "Comanche 18" (Sub-Atlantic, UK) was used, equipped with manipulators and samplers for collecting bottom sediments and geological samples. The surface layer (0–3 cm) of sediment was collected with the apparatus net; short cores of sediment were taken using plastic tubes with a diameter of 48 mm, followed by cutting into layers of 1 cm or 3 cm (Table 1).

2.2. Sample preparation of radiolarians

The samples were prepared for radiolarian studies according the methods described by Lipman (1979) and Tochilina (1985). Canada Balsam DC (refractive index = 1.520–1.523) was used to prepare the slides. The radiolarian skeletons were studied using a LOMO Mikmed 6 Microscope (300× magnification, St. Petersburg, Russia). We calculated the total radiolarian content (TRC) (the number of radiolarian skeletons per gram of air-dry sediment) (Vasilenko and Vasilenko, 2021), the number of species and percentages of each species in assemblages. TRC $= (n \times w_f)/(w_s \times w_p)$, where n is the number of skeletons on the slide; w_f is the weight of the >40 μm fraction (gram); w_s is the weight of the air-dry sediment (gram); w_p is the weight of portion of the >40 μm fraction (gram). The radiolarians were photographed under transmitted light using the Touptek photonics FMA050 digital camera (Hangzhou, China). The taxonomic framework used closely follows that of Tochilina (1996), Tochilina and Vasilenko (2018), and Afanasieva and Amon (2006) for the stauraxon radiolarians of the class Stauraxonaria. The radiolarian species were identified from the following main sources: Bailey (1856), Haeckel (1862, 1887), Hays (1970), Lazarus et al. (2005) and Takahashi (1991). In the Results we presented only dominant and subdominant species in radiolarian assemblages. The full taxonomic composition is given in Table S1.

2.3. Sample preparation of diatoms and silicoflagellates

The sediment treatment for microscopy, as well as estimation of the diatom content in sediments (valves per gram of the air-dry sediment) were conducted based on standard procedures (Jousé et al., 1974). The samples were enriched with a potassium-cadmium liquid (H_2O:Cd_2:KI = 1:2.5:2.25) with a density of 2.6. Samples were processed only with distilled water. Unenriched sediment was used to determine the concentration of diatoms in sediments. For the preparation of slides, a highly refractive MOUNTEX resin (refractive index 1.67) (Darmstadt Germany) was used. The diatoms were identified and enumerated with an IMAGER.A1 light microscope (magnification = ×1000; Carl Zeiss AG, Oberkochen Germany) and imaged with an AxioCamMrC digital video camera (Carl Zeiss AG). Total of 100–200 specimens were counted in each sample to determine the percentage of diatom species in assemblages. The surface sediment diatom temperature index (Td) was applied to estimate the influence of temperatures on changes in diatom assemblages from north to south. Td= (Xw/Xw + Xc), where Xw is the percentage of warm-water (tropical and subtropical) diatoms and Xc (arctic, boreal) that of cold-water and temperate diatoms (Koizumi, 1986).

The diatoms and silicoflagellates were identified from the following sources: Bukry and Foster (1973), Chang et al. (2017), Desikachary and Prema (1996), Garcia and Odebrecht (2012), Hasle and Syversten (1997), Hernandez-Becerril and Bravo-Sierra (2001), Jordan and McCartney (2015), Jousé and Kazarina (1974), Kozyrenko et al. (2008), Makarova et al. (2002), Poelchau (1976), Round et al. (1990), and Takahashi (1987). Ecological and biogeographic characteristics of diatoms are after Jousé et al. (1969), Ren et al. (2014), Romero et al. (2005), Semina (1974), and Tanimura et al. (2007).

3. Results

3.1. Radiolarians

3.1.1. Concentration of radiolarians in sediments

The TRC in the sediments varied widely (Fig. 2). In the upper bathyal zone of the slope of Koko Guyot (777 m), radiolarians are rare in surface

Table 1
Site locations in the Emperor Seamount Chain and types of sediment samples collected during the 86th (2019) and 94th (2020) cruises RV *Akademik M.A. Lavrentyev*.

Guyot	Site	Latitude (N)	Longitude (E)	Depth (m)	Sample	Sediment type
Nintoku	LV86-21	40.9992	170.7247	1161	LV86-21 (0–3 cm)	Silty foraminiferal ooze
Jingu	LV86-12	38.7736	171.0872	1935	LV86-12 (0–3 cm)	Silty foraminiferal ooze
					LV86-12 (12–15 cm)	Silty foraminiferal ooze
					LV86-12 (18–21 cm)	Silty foraminiferal ooze
	LV86-14	38.7624	171.0857	1446	LV86-14 (0–3 cm)	Silty foraminiferal ooze
					LV86-14 (12–15 cm)	Silty foraminiferal ooze
					LV86-14 (24–27 cm)	Silty foraminiferal ooze
Ojin	LV86-18	38.0333	170.2139	1531	LV86-18 (0–3 cm)	Silty foraminiferal ooze
Koko	LV86-5	35.6033	171.2230	777	LV86-5 (0–3 cm)	Clayey foraminiferal ooze
					LV86-5 (12–15 cm)	Clayey foraminiferal ooze
	LV86-6	35.7840	171.0649	1995	LV86-6 (0–3 cm)	Silty foraminiferal ooze
	LV86-11	35.0725	171.2884	1880	LV86-11 (0–3 cm)	Silty foraminiferal ooze
					LV86-11 (12–15 cm)	Silty foraminiferal ooze
	LV86-17	35.0945	171.3182	1440	LV86-17 (0–3 cm)	Silty foraminiferal ooze
	LV94-12	35.789	171.048	2231–2242	LV94-12-K2-2 (1–2 cm)	Silty foraminiferal ooze
					LV94-12-K2-3 (2–3 cm)	Silty foraminiferal ooze
					LV94-12-K2-4 (3–4 cm)	Silty foraminiferal ooze
					LV94-12-K2-5 (4–5 cm)	Silty foraminiferal ooze
					LV94-12-K2-6 (5–6 cm)	Silty foraminiferal ooze
					LV94-12-K2-7 (6–7 cm)	Silty foraminiferal ooze
					LV94-12-K2-8 (7–8 cm)	Silty foraminiferal ooze
					LV94-12-K2-9 (8–9 cm)	Silty foraminiferal ooze
Yuryaku	LV94-7	32.53	172.30	1249	LV 94-7-K7-1 (0–1 cm)	Foraminiferal sand
					LV 94-7-K7-2 (1–2 cm)	Foraminiferal sand
					LV 94-7-K7-3 (2–3 cm)	Foraminiferal sand
	LV94-10	32.53	172.29	1243–1249	LV94-10-2-K3-2 (1–2 cm)	Foraminiferal sand
					LV94-10-4-K2-1 (0–1 cm)	Foraminiferal sand

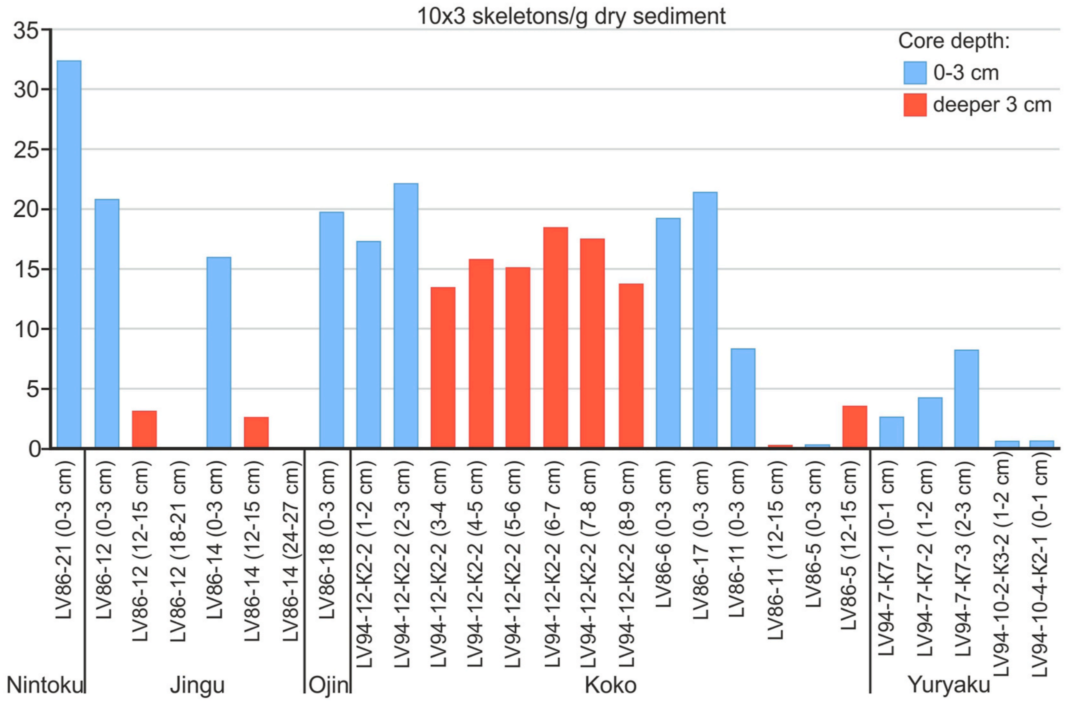

Fig. 2. Concentration of radiolarians (skeletons per gram dry sediment) in the surface sediments of the ESC guyots.

sediments (interval 0–3 cm), but below (12–15 cm) the TRC and taxonomic diversity increased. A large number of radiolarians (mainly 15000-32361 skeletons per gram) were contained in the upper 3 cm of the lower bathyal zone (1161–2242 m) of the Nintoku, Jingu, Ojin, and Koko guyots. With increasing core depth, the TRC in sediments sharply decreased (12–15 cm), up to their complete disappearance (18–27 cm; Fig. 2). A low number of radiolarians were noted in the sediments of the Yuryaku Guyot, which are represented by foraminiferal sands.

3.1.2. *Radiolarian assemblages*

A diverse radiolarian fauna was found: 104 taxa from 68 genera of Spumellaria, 120 taxa from 61 genera of Nassellaria, and 13 taxa from 7 genus of Collodaria. The radiolarian fauna of surface sediments of the Nintoku Guyot is characterized by 68 taxa (Table S1) and the maximum TRC (32361 skeletons per gram). It consists of almost equal numbers of subtropical and tropical (51%) and arctic-boreal (49%) species. Arctic-boreal radiolarians are represented by the species *Botryostrobus aquilonaris* (5.8%), *Lithelius minor* (3.9%), *Actinomma delicatulum* (2.4%), *Actinomma leptodermum* (1.9%), and *Spurioclathrocyclas bicornis* (1.4%,

Table S1). Most of them were found in sediments of other guyots we studied, except for *Stichopilium bicorne*, which was found only in sediments of Nintoku Guyot. The composition of subtropical and tropical species is also wide; there is no sharp dominance of any taxa. Representatives of the genera *Photricium* (10%), *Tetrapyle* (5.3%), and species *Cenosphaer*a sp. F.1 (3.9%), *Theoconus junonis* (2.9%), *Hexastylus dimensivus* (1.9%), *Actinomma medianum* (1.4%) were identified. *Botryostrobus aquilonaris, Axoprunum bispiculum,* and *Spurioclathrocyclas bicornis* live in the boreal and subtropical northwestern Pacific between 200 and 3000 m (Kling and Boltovskoy, 1995; Okazaki et al., 2004, 2005; Matsuzaki et al., 2020). *Pseudodictyophimus gracilipes* and *Tetrapyle octacantha* live at greater depths in low latitudes (Ishitani and Takahashi, 2007).

On the Jingu Guyot, the largest TRC (15941-20790 skeletons per gram) was recorded between 0 and 3 cm, but deeper that it sharply decreased, probably due to dissolution and the action of bottom currents (Fig. 2). The ratio of subtropical and tropical (51–55%) and arctic-boreal (45–48%) species is approximately the same as in the sediments of the Nintoku Guyot. Arctic-boreal radiolarians are represented by the taxa listed above with some variations in their abundance (Fig. 3). In addition, *Sethodiscus macrococcus* (6.7%), *Spongopyle osculosa* (1.4%), *Stylosphaera lithatractus* (0.9%) were found. Among subtropical and tropical species, the content of *Tetrapyle* (8.1–12.2%) and *Photricium* (8.4–9.1%) also increase. *Heliodiscus asteriscus* (0.5–6.7%), *Larcospira quadrangula* (0.5–2.9%), *Dictyoceras virchowii* (6.6%) were found.

The assemblage contains species that inhabits depths <200 m (*Ommatartus tetrathalamus, Tetrapyle octacantha, Larcospira quadrangula, Spongaster tetras tetras, Spongocore puella,* etc.), and deep-sea species that

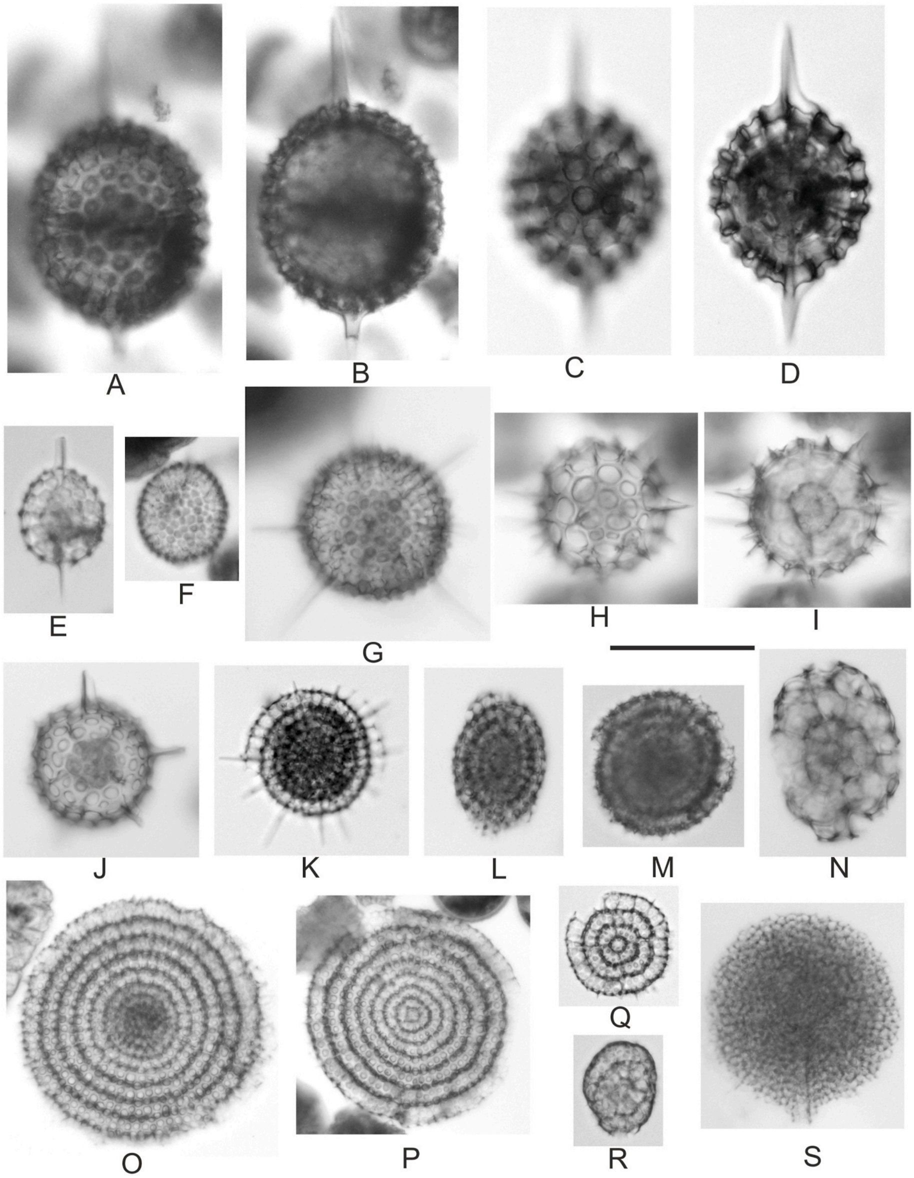

Fig. 3. Arctic-boreal, boreal, and subtropical radiolarians (Spumellaria) from sediments of the ESC guyots: **A, B** – *Axoprunum bispiculum* (Popofsky) – one specimen at various foci, sample LV94-12-K2-9 (8–9 cm). **C, D** – *Stylosphaera lithatractus* Haeckel – one specimen at various foci, sample LV94-7K7-2 (1–2 cm). **E** – *Druppatractus pyriformis* (Bailey), sample LV94-12-K2-5 (4–5 cm). **F** – *Druppatractus irregularis* Popofsky, sample LV94-12-K2-6 (5–6 cm). **G** – *Actinomma delicatulum* (Dogiel), sample LV86-14 (0–3 cm). **H, I** – *Actinomma leptodermum* (Jørgensen) – one specimen at various foci, sample LV86-17 (0–3 cm). **J** – *Hexacontium pachydermum* Jørgensen, sample LV86-12 (0–3 cm). **K** – *Spirotunica spiralis* (Haeckel), sample LV94-7K7-1 (0–3 cm). **L** – *Larcopyle weddellium* Lazarus, Faust, Popova, sample LV86-14 (0–3 cm). **M** – *Lithelius minor* Jørgensen, sample LV94-7K7-3 (2–3 cm). **N** – *Larcopyle bütschlii* Dreyer, sample LV94-7K7-1 (0–3 cm). **O** – *Stylodictya tenuispina* Jørgensen, sample LV86-11 (0–3 cm). **P** – *Stylodictya validispina* Jørgensen, sample LV86-17 (0–3 cm). **Q** – *Stylodictya stellata* Bailey, sample LV86-18 (0–3 cm). **R** – *Larcopyle labyrinthusa* Lazarus, Faust, Popova, sample LV86-18 (0–3 cm). **S** – *Spongopyle osculosa* Dreyer, sample LV86-14 (0–3 cm). Scale bars = 100 μm.

inhabit depths >500 m (*Saturnalis circularis, Hexacontium pachydermum, Actinomma leptodermum, Cycladophora davisiana* (Okazaki et al., 2005; Ishitani and Takahashi, 2007; Matsuzaki and Itaki, 2017; Matsuzaki et al., 2020).

The radiolarian assemblage from the surface sediments of the Ojin Guyot differs substantially from those described above by a decrease in the number of arctic-boreal (33%) and an increase in the number of subtropical and tropical (64%) species. TRC = 19732 skeletons per

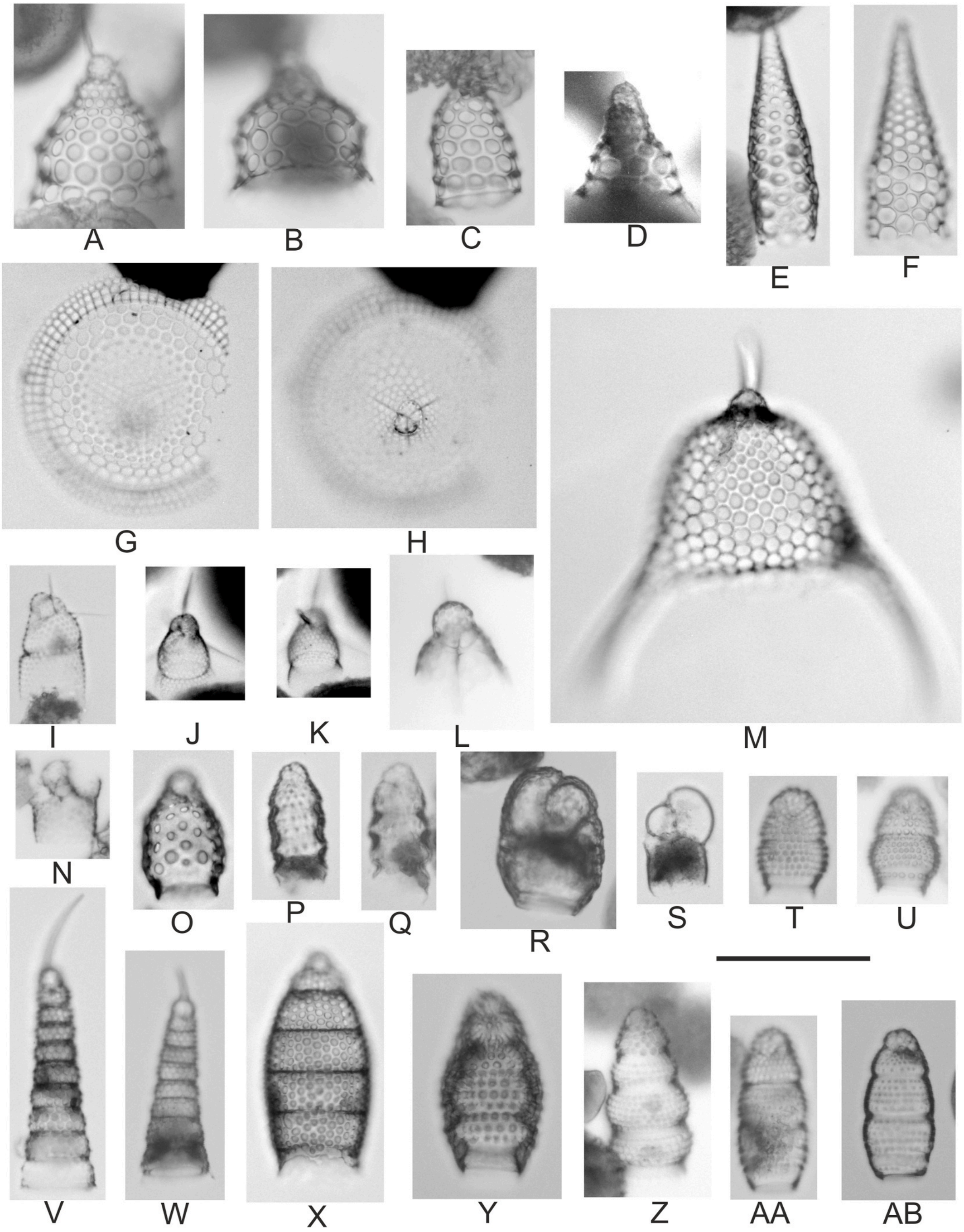

Fig. 4. Arctic-boreal, boreal, and subtropical radiolarians (Nassellaria) from sediments of the ESC guyots: **A** – *Spurioclathrocyclas bicornis* (Popofsky), sample LV86-21 (0–3 cm). **B** – *Spurioclathrocyclas parabicornis* (Hays) Tochilina et Vasilenko, sample LV86-21(0–3 cm). **C** – *Cycladophora cornuta* (Bailey), sample LV86-18 (0–3 cm). **D** – *Cycladophora davisiana* Ehrenberg, sample LV94-12-K2-9 (8–9 cm). **E** – *Cornutella bimarginata* Haeckel, sample LV86-18 (0–3 cm). **F** – *Cornutella profunda* Ehrenberg, sample LV86-18 (0–3 cm). **G, H** – *Eucecryphalus sestodiscus* (Haeckel) – one specimen at various foci, sample LV94-12-K2-2 (1–2 cm). **I–K** – *Artobotrys borealis* Cleve, **I** – sample LV94-12-K2-5 (4–5 cm), **J, K** – one specimen at various foci, sample LV94-12-K2-7 (6–7 cm). **L** – *Pseudodictyophimus gracilipes* (Bailey), sample LV86-12 (0–3 cm). **M** – *Dictyopodium trilobum* Haeckel, sample LV94-12-K2-3 (2–3 cm). **N** – *Amphimelissa setosa* (Cleve), sample LV86-6 (0–3 cm). **O** – *Carpocanarium papillosum* (Ehrenberg), sample LV86-18 (0–3 cm). **P, Q** – *Siphocampe arachnea* (Ehrenberg), **P** – sample LV94-12-K2-8 (7–8 cm), **Q** – sample LV94-12-K2-5 (4–5 cm). **R** – *Botryocampe robusta* (Kruglikova), sample LV86-21 (0–3 cm). **S** – *Botryocampe inflata* (Bailey), sample LV94-12-K2-9 (8–9 cm). **T, U** – *Botryostrobus* cf. *tumidulum* Bailey, **T** – sample LV94-12-K2-5 (4–5 cm), **U** – sample LV86-12 (0–3 cm). **V, W** – *Cyrtopera languncula* Haeckel, **V** – sample LV94-12-K2-2 (1–2 cm), **W** – sample LV94-12-K2-3 (2–3 cm). **X** – *Eucyrtidium acuminatum* (Ehrenberg), sample LV86-21 (0–3 cm). **Y** – *Botryostrobus aquilonaris* (Bailey), sample LV86-21 (0–3 cm). **Z** – *Botryostrobus auritus* (Ehrenberg), sample LV86-11 (0–3 cm). **AA, AB** – *Lithocampe* ex gr. *platycephala* (Ehrenberg), **AA** – sample LV94-12-K2-5 (4–5 cm), **AB** – sample LV86-18 (0–3 cm). Scale bars = 100 μm.

gram. Arctic-boreal radiolarians are represented by *Larcopyle weddellium* (3.5%), *Botryostrobus aquilonaris* (3.5%), *Botryostrobus auritus* (2.6%), *Actinomma leptodermum* (2.2%; Fig. 4). For the first time, the presence of colonial species was noted: *Acrosphaera spinosa* (0.9%), *Siphonosphaera abyssi* (0.9%), *Clathrosphaera circumtexta* (0.4%; Fig. 5). Also, the assemblage contains species *Pterocanium praetextum praetextum* (1.7%), *Eucyrtidium hexastichum* (0.9%), *Pterocorys sabae* (0.4%). These species have not been found in the sediments of the Nintoku and Jingu guyots.

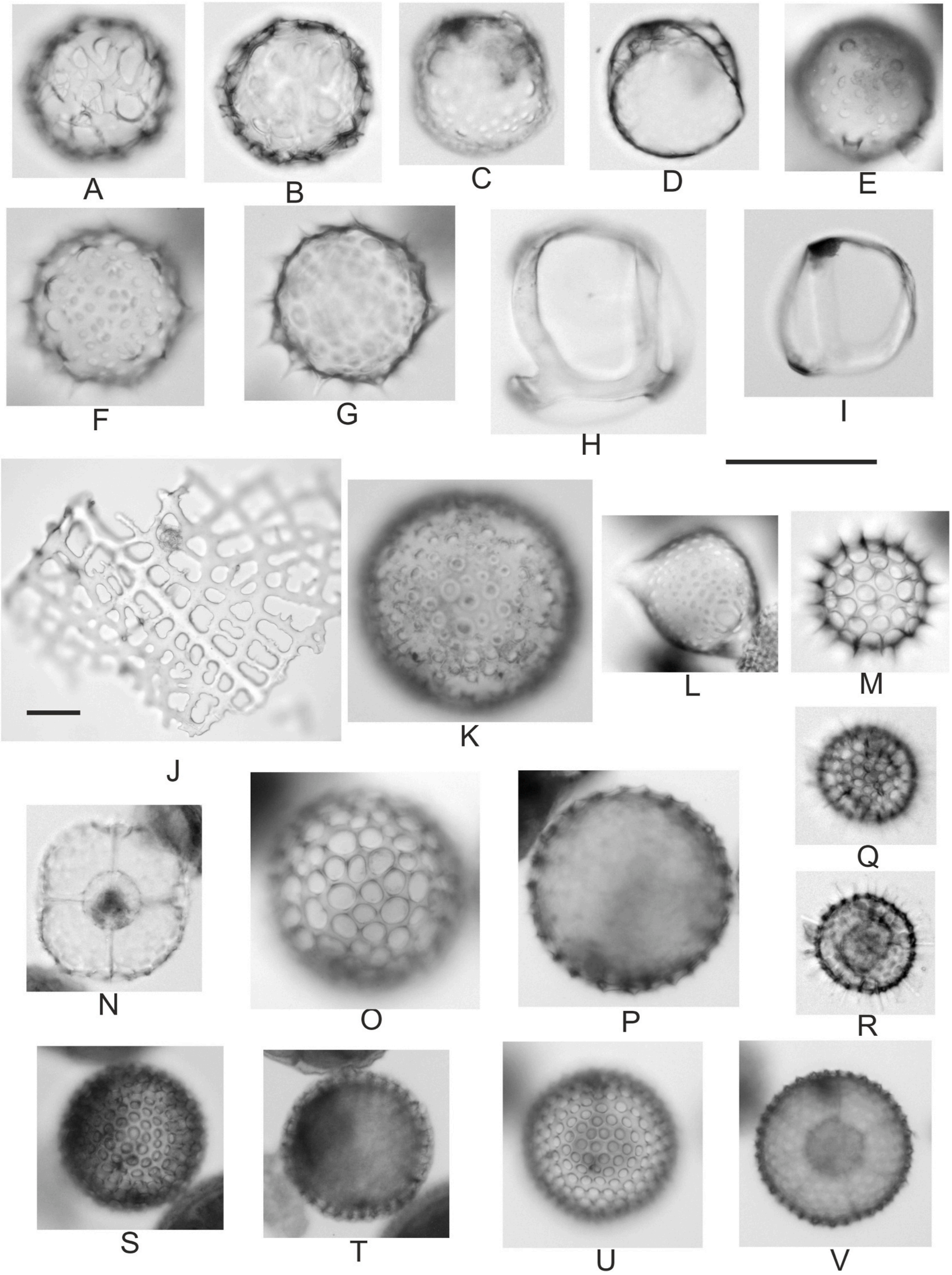

Fig. 5. Tropical and subtropical radiolarians (Collodaria and Spumellaria) from sediments of the ESC guyots: **A, B** – *Clathrosphaera circumtexta* Haeckel – one specimen at various foci, sample LV86-18 (0–3 cm). **C, D** – *Collosphaera tuberosa* Haeckel – one specimen at various foci, sample LV94-12-K2-4 (3–4 cm). **E** – *Siphonosphaera abyssi* (Ehrenberg), sample LV94-12-K2-4 (3–4 cm). **F, G** – *Acrosphaera spinosa* (Haeckel) – one specimen at various foci, sample LV94-12-K2-4 (3–4 cm). **H, I** –*Collosphaera macropora* Popofsky, **H** –sample LV94-12-K2-3 (2–3 cm). **i** – sample LV94-12-K2-7 (6–7 cm). **J** – *Orosphaera hyxleyii* Haeckel – fragment, sample LV94-12-K2-6 (5–6 cm). **K** – *Collosphaera confossa* Takahashi, sample LV94-12-K2-3 (2–3 cm). **L** – *Otosphaera* cf. *polymorpha* Haeckel, sample LV94-12-K2-2 (1–2 cm). **M** – *Cladococcus* cf. *cervicornis* Haeckel, sample LV86-18 (0–3 cM). **N** – *Stylosphaera melpomene* Haeckel, sample LV94-12-K2-4 (3–4 cm). **O, P** – *Cenosphaera* sp. F.1 – one specimen at various foci, sample LV86-6 (0–3 cm). **Q, R** – *Haliomma* (?) sp. – one specimen at various foci, sample LV94-12-K2-7 (6–7 cm). **S, T** – *Cenosphaera* sp. F.2 – one specimen at various foci, sample LV86-18 (0–3 cm). **U, V** – *Thecosphaera greccoi* Vinassa de Regny – one specimen at various foci, sample LV86-11 (0–3 cm). Scale bars = 100 μm.

Ecological characteristics of species also indicate the presence of both surface–subsurface and deep-water species living in waters <3000 m (Table S1). According to Motoyama and Nishimura (2005), the northern boundary of the species *Siphonosphaera abyssi* (species of the *Siphonosphaera* spp. group), *Disolenia quadrata* (identified as *Trisolenia* spp.), *Pterocanium praetextum praetextum* and *Theocorythium trachelium* is at the Kuroshio Bifurcation Front. Those data coincide with ours, except for the species *Theocorythium trachelium*, which was also found further north in the Jingu and Nintoku guyots.

The most diverse radiolarians were found in the sediments of the Koko Guyot (Table S1). At 2242 m a rich radiolarian fauna was found (TRC = 13424-22069 skeletons per gram; taxonomic composition = 97-117 taxa) (Table S1). High abundance of radiolarians and rich taxonomic composition are observed along the entire length of the core, with a sharp drop in TRC between 3-4 and 8–9 cm (Fig. 6). In surface sediments at 1440–1995 m, the taxonomic composition is less diverse; 35–75 taxa, and the TRC reaches 8277–21336 skeletons per gram. The lowest TRC was found in sediments from 777 m. The surface sediments of core LV86-5 contain only one species of *Tetrapyle octacantha*, but between 12 and 15 cm there were 9 taxa: *Actinomma leptodermum, Tetrapyle octacantha, Larcospira quadrangular, Tholospyra* (?) sp., *Lithelius minor*, *Phorticium* spp., *Dictyocoryne* sp., *Clathrocorys* sp., and *Botryostrobus aquilonaris*.

In the sediments of Koko Guyot the content of arctic-boreal species sharply decreases (21–30%), while subtropical and tropical species become more diverse and numerous (70–76%). Among arctic-boreal radiolarians, relatively high concentrations are reached by the species *Lithelius minor* (1.0–10.1%), *Stylodictya validispina* (2.4–5.8%), *Botryostrobus auritus* (1.0–3.8%). Samples LV94-12-K2 (7–8 cm), LV86-6 (0–3 cm), and LV86-17 (0–3 cm) contain *Amphimelissa setosa*, which, according to Ikenoue et al. (2016) and Matsuzaki and Suzuki (2018) migrated to the Arctic 0.085–0.04 Ma.

Tropical and subtropical radiolarians are represented by the above-mentioned species, as well as species not found in the sediments of the other guyots: *Carpocanium ruesti* (2.6%), *Carpocanistrum acephalum* (0.3–1.6%), *Staurotholus dodecastylus* (0.3–1.1%), *Tholoma metallason* (0.3–0.8%, Figs. 7–9). The content species of the genera *Tetrapyle* (10.9–19.2%), *Photricium* (2.1–10.9%). The diversity of species Collodaria are increase significantly compared to the assemblages described above (Table S1). These species are widespread in the transitional, subtropical and tropical zones of the Pacific, while they are absent in the arctic-boreal zone (Takahashi, 1991; Motoyama, Nishimura, 2005; Kamikuri et al., 2008; Matsuzaki and Itaki, 2017). They also live in a wide depth range (0–3000 m; Table S1).

On the Yuryaku Guyot, sediments from 1249 m are represented by foraminiferal sands, which contain a low number of radiolarians, and species diversity is also decreased. At site LV94-10, 10 taxa of radiolarians were identified, represented by subtropical and tropical species (Table S1). TRC = 667–683 skeletons per gram.

Core LV94-7K7 showed an increase in TRC with depth from 2681 skeletons per gram (0–1 cm) to 8254 skeletons per gram (2–3 cm) (Table S1, Fig. 2). Diversity also increases from 20 to 48 taxa, respectively. The composition is dominated by subtropical and tropical species (up to 78%), the same as in the sediments of the Koko Guyot. These include colonial species *Siphonosphaera abyssi* (3.8–4.1%), *Acrosphaera spinosa* (3.1–3.8%), *Collosphaera macropora* (1.0%), and tropical taxa *Heliosoma* sp. (2.8%), *Xiphatractus* cf. *cronos* (1.9%), *Stomatosphaera* sp. (1.0%), *Botryocyrtis quinaria* (1.0%; Fig. 9), which were not found in the assemblages described above. The content of arcto-boreal species drops to 21%. Among them, *Lithelius minor* (3.8–10.2%), *Stylodictya validispina* (3.1–5.8%), *Spirotunica spiralis* (1.9–5.6%), and *Larcopyle bütschlii* (1.0–5.6%) has a high content. Due to the small number of specimens in the preparations, the percentage of each taxon may be overestimated.

3.2. Diatoms

3.2.1. Concentrations of diatoms in sediments

The content of diatoms (number of valves per gram air-dried sediment) in surface sediments is uneven (Fig. 10). The maximum content (2.83 mln valves per gram) was found in sediments of the northernmost site of Koko Guyot. A noticeable concentration of diatoms was noted in the sediments of the Jingu Guyot – 1.11 mln valves per gram and Nintoku Guyot– 0.66 mln valves per gram. At other sites, the content of diatoms is very low (0.26–0.03 mln valves per gram) to almost complete absence in the sediments of the Yuryaku Guyot. The content of diatoms in the lower parts of the cores on the Jingu (12–21 and 24–27 cm) and Koko (12–15 cm) guyots drops sharply (to 0.01–0.07 mln valves per gram).

3.2.2. Diatom assemblages

In surface sediments of the southern ESC guyots, 60 species and infraspecific taxa of diatoms belonging to 29 genera have been identified (Table S2). The largest number of species is characteristic of the genera *Coscinodiscus* (6 species and infraspecific taxa), *Actinocyclus* (6), *Thalassiosira* (6), *Azpeitia* (4), *Thalassionema* (4), *Nitzschia* (3).

The diatom assemblages are characterized by a predominance of warm-water species *Fragilariopsis doliolus*, *Azpeitia nodulifera*, *A. africana*, *Thalassiosira leptopus*, *Alveus marinus*, *Actinocyclus cuneiformis*, *Roperia tesselata* (Figs. 11 and 12). as well as species of *Rhizosolenia bergonii*, *Thalassiosira lineata*, rare species of *Pseudosolenia calcar-avis*, *Brightwellia mirabilis*, *Cestodiscus cinnamomeus*, *Nitzschia kolaczeckii*, and *N. bicapitata* (Table S2), characteristic of waters of subtropical and tropical latitudes (Jousé, 1977; Jousé et al., 1969; Round et al., 1990; Kaczmarska and Fryxell, 1996; Hasle and Syversten, 1997; Garcia and

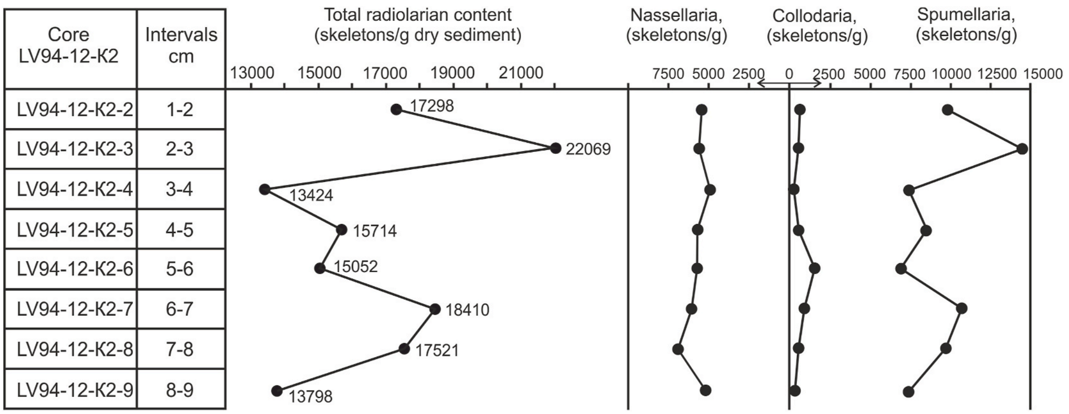

Fig. 6. Changes in the total radiolarian content and quantitative ratios of high-rank radiolarian taxa (Spumellaria, Nassellaria, and Collodaria) in the sediments of Core LV94-12-K2.

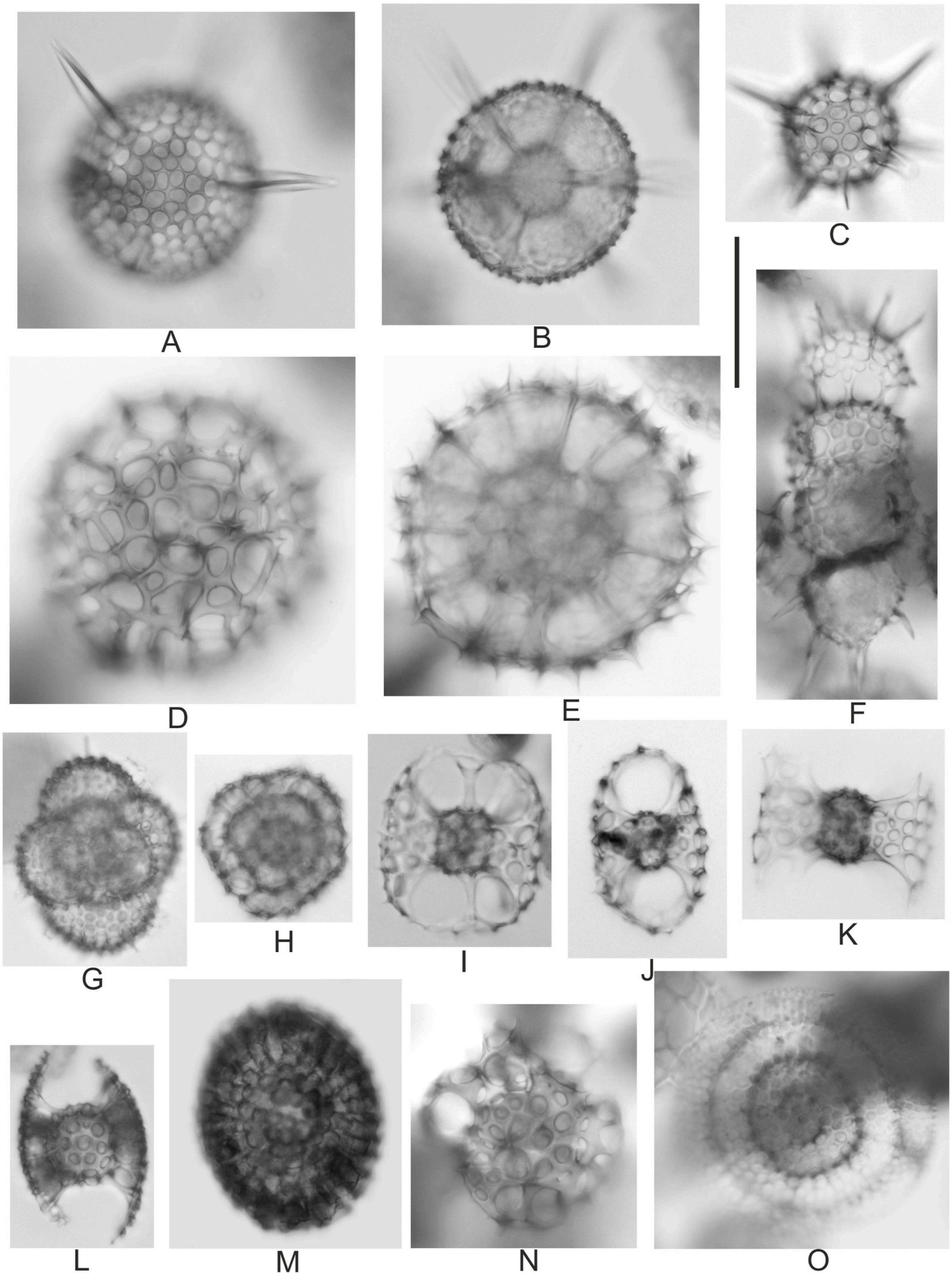

Fig. 7. Tropical and subtropical radiolarians (Spumellaria) from sediments of the ESC guyots: **A, B** – *Hexastylus dimensivus* Haecke l– one specimen at various foci, sample LV86-18 (0–3 cm). **C** – *Actinomma* spp., sample LV86-21 (0–3 cm). **D, E** – *Actinomma medianum* Nigrini – one specimen at various foci, sample LV86-6 (0–3 cm). **F** – *Panicium coronatum* Haeckel, sample LV94-12-K2-4 (3–4 cm). **G** – *Staurotholus* cf. *dodecastylus* Haeckel, sample LV94-12-K2-4 (3–4 cm). **H** – *Tholospyra* spp., sample LV86-12 (0–3 cm). **I** – *Octopyle stenozona* Haeckel, sample LV94-12-K2-4 (3–4 cm). **J** – *Tetrapyle quadrilobum* Ehrenberg, sample LV86-11 (0–3 cm). **K** – *Tetrapyle octacantha* Müller, sample LV86-17 (0–3 cm). **L** – *Sethodiscus macrococcus* Haeckel, sample LV94-12-K2-3 (2–3 cm). **M** – *Prunopyle burbachii* Dreyer, sample LV94-7K7-1 (0–3 cm). **N** – *Phorticium* spp., sample LV86-17 (0–3 cm). **O** – *Circodiscus microporus* (Stöhr), sample LV94-12-K2-3 (2–3 cm). Scale bars = 100 μm.

Odebrecht, 2012; Ren et al., 2014).

In all samples, the abundance of representatives of the genus *Thalassionema* (*T. frauenfeldii*, *T. nitzschioides*, *T. nitzschioides* var. *parvum*) is large (Figs. 11 and 13), as they are widespread in shelf and oceanic waters from tropical to temperate latitudes (Semina, 1974; Konovalova et al., 1989). The species *Thalassionema nitzschioides* and its warm-water morphological type *T. nitzschioides* var. *parvum* are particularly abundant in sediments under the Kuroshio Front and under the Subarctic Gyre in the North Pacific (Tanimura et al., 2007).

The diatom flora in the samples from the sediments of ESC guyots consisted of predominantly of planktonic species (58 species), of which the majority are oceanic (34 taxa), which dominate abundance (Fig. 14). The remaining species are neritic-oceanic or panthalassic (11 taxa) and neritic (9 taxa) species. Almost all diatom assemblages contain the

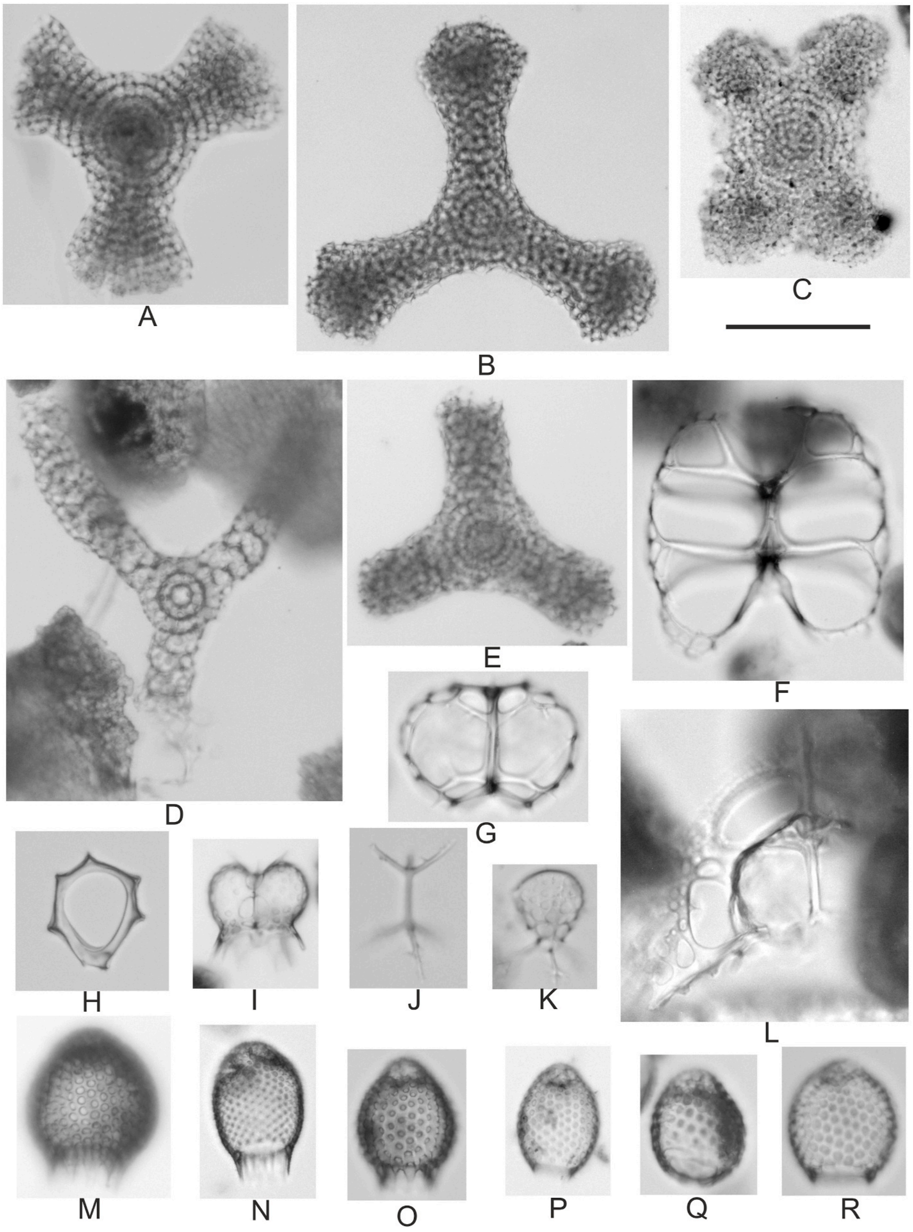

Fig. 8. Tropical and subtropical radiolarians (Spumellaria and Nassellaria) from sediments of the ESC guyots: **A** – *Euchitonia triangulum* (Ehrenberg), sample LV94-12-K2-2 (1–2 cm). **B** – *Euchitonia mulleri* Haeckel, sample LV94-7K7-2 (1–2 cm). **C** – *Spongaster tetras irregularis* Nigrini, sample LV94-7K7-3 (2–3 cm). **D** – *Euchitonia elegans* Ehrenberg, sample LV94-12-K2-5 (4–5 cm). **E** – *Euchitonia pacifica* Ehrenberg, sample LV86-17 (0–3 cm). **F** – *Liriospyris reticulata* (Ehrenberg), sample LV94-12-K2-2 (1–2 cm). **G** – *Lophospyris chenii* Goll, sample LV94-12-K2-3 (2–3 cm). **H** – *Archicircus primordialis* Haeckel, sample LV94-12-K2-2 (1–2 cm). **I** – *Phormospyris stabilis capoi* Goll, sample LV86-17 (0–3 cm). **J** – *Tetraplecta* sp., sample LV94-12-K2-2 (1–2 cm). **K** – *Peridium spinipes* Haeckel, sample LV94-12-K2-4 (3–4 cm). **L** – *Clathrocorys murrayi* Haeckel, sample LV94-12-K2-3 (2–3 cm). **M** – *Carpocanium pachydermicum* Chen & Tan, sample LV86-6 (0–3 cm). **N** – *Carpocanistrum acephalum* Haeckel, sample LV86-17 (0–3 cm). **O** – *Carpocanium flosculum* Haeckel, sample LV86-21 (0–3 cm). **P** – *Carpocanistrum acutidentatum* Takahashi, sample LV94-7K7-2 (1–2 cm). **Q** – *Carpocanium prunoides* Popofsky, sample LV94-12-K2-2 (1–2 cm). **R** – *Carpocanium obliquum* (Haeckel), sample LV94-12-K2-4 (3–4 cm). Scale bars = 100 μm.

tychopelagic species *Actinoptychus senarius* and *Paralia sulcata*, which are found in both the benthos and plankton and are characteristic mainly of shelf sediments. The content of the latter species reaches 5.6% in sediments of the Koko Guyot. On the Nintoku Guyots, and Koko there is a single benthic species *Diploneis weissflogii*. In addition, 3 fossil species were found in the sediments: *Craspedodiscus coscinodiscus*, which became extinct at the end of the Middle Miocene in the equatorial Pacific (Barron, 2003), *Azpeitia vetustissima*, extinct in the early Late Miocene (Tsoy and Shastina, 1999) and *Proboscia barboi*, extinct in the Pleistocene (Pushkar and Cherepanova, 2001).

Warm-water (tropical and subtropical) species predominated, both in number of species (25 taxa) and abundance (52.5–86%). Most warm-water species (*Fragilariopsis doliolus*, *Azpeitia nodulifera*, *Thalassiosira leptopus*, *Alveus marinus*, *Actinocyclus cuneiformis*, *Roperia tesselata*, *Rhizosolenia bergonii* et al.) were distributed in areas with maximum summer temperatures of 16–27 °C and are characteristic of the Subtropical factor, the influence of which is strongest in the zone of influence of the warm Kuroshio Current and the North Pacific Current (Ren et al., 2014). Cold-water species are represented by 17 species (*Coscinodiscus marginatus*, *Neodenticula seminae*, *Rhizosolenia hebetata*, *Actinocyclus curvatulus*, *Proboscia subarctica*, *Thalassiothrix longissima*, *Thalassiosira antarctica*, *Shionodiscus latimarginatus* et al.), characteristic of the

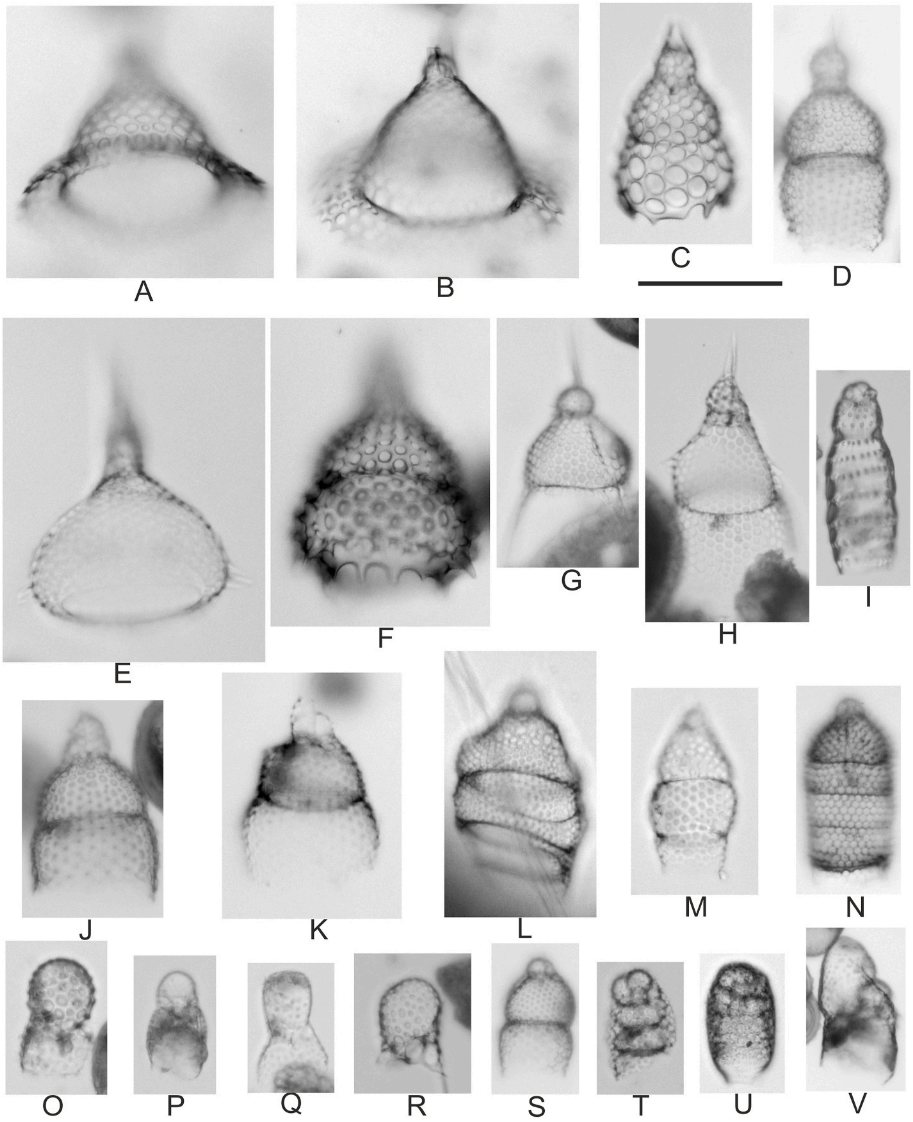

Fig. 9. Tropical and subtropical radiolarians (Nassellaria) from sediments of the ESC guyots: **A**, **B** *Eucecryphalus cervus* (Ehrenberg) – one specimen at various foci, sample LV86-14 (0–3 cm). **C** – *Theoconus junonis* Haeckel, sample LV86-21 (0–3 cm). **D** – *Theocorythium trachelium* (Ehrenberg), sample LV86-11 (0–3 cm). **E** – *Anthocyrtidium cineraria* Haeckel, sample LV94-12-K2-7 (6–7 cm). **F** – *Lamprocyclas maritalis* Haeckel, sample LV86-12 (0–3 cm). **G** – *Pterocanium praetextum praetextum* (Ehrenberg), sample LV94-12-K2-5 (4–5 cm). **H –** *Pterocorys sabae* (Ehrenberg), sample LV94-12-K2-3 (2–3 cm). **I** – *Siphocampium cylindrica* Haeckel, sample LV86-21 (0–3 cm). **J** – *Pterocorys zancleus* (Müller), sample LV86-21 (0–3 cm). **K** – *Dictyoceras virchowii* Haeckel, sample LV86-6 (0–3 cm). **L** – *Eucyrtidium anomalum* (Haeckel), sample LV86-17 (0–3 cm). **M** – *Theocyrtis* sp., sample LV94-12-K2-2 (1–2 cm). **N** – *Eucyrtidium hexacola* (Haeckel), sample LV86-11 (0–3 cm). **O** – *Botryopera babayagae* Trubovitz, sample LV94-12-K2-6 (0–3 cm). **P** – *Lithomelissa setosa* Jørgensen, sample LV94-12-K2-6 (0–3 cm). **Q** – *Lophophaena* sp., sample LV94-12-K2-4 (3–4 cm). **R** – *Dimelissa thoracites* (Haeckel), sample LV94-12-K2-2 (1–2 cm). **S** – *Theocorys veneris* Haeckel, sample LV86-17 (0–3 cm). **T** – *Botryocyrtis scutum* (Harting), sample LV94-7K7-3 (2–3 cm). **U** – *Botryocyrtis quinaria* Ehrenberg, sample LV94-7K7-3 (2–3 cm). **V** – *Lithobotrys cribrosa* Ehrenberg, sample LV86-17 (0–3 cm). Scale bars = 100 μm.

Subarctic Pacific Ocean (Kazarina and Yushina, 1999; Tsoy and Wong, 1999; Kozyrenko et al., 2008) with summer maximum surface temperatures water 6.5–15 °C (Ren et al., 2014). Their substantial abundance was noted in diatom assemblages from sediments of the Nintoku (33%) and Jingu (11.5–19.5%) guyots, which distinguishes these from the Ojin, Koko, and Yuryaku guyots, located south of 38°N. The values of the diatom temperature index (Td), which reflects the ratio of warm-water and cold-water species in diatom assemblages, increased from 0.61 to 0.87 for the Nintoku-Jingu assemblages to 0.95–0.99 for the Ojin-Koko-Yuryaku assemblages (Fig. 15). The differences between the Nintoku-Jingu diatom assemblages, formed under the influence of the Subarctic waters, and the Ojin-Koko-Yuryaku ones, influenced by the Subtropical waters, are clear.

3.3. Silicoflagellates

Silicoflagellates were found in sediments of all guyots; their abundance was uneven and decreased from north to south (Table S2). They are represented by 5 species belonging to 3 genera. The warm-water species *Dictyocha messanensis*, *D. fibula* and the moderate-cold-water species *Dictyocha epiodon* (Fig. 16) are found in sediments of all guyots except Yuryaku Guyot. The cold-water species *Stephanocha octangulata* and *Octactis speculum* are found mainly in sediments of the northern Nintoku and Jingu guyots. Deep-sea drilling in the surface sediments of Nintoku Guyot (DSDP Site 432) revealed only rare specimens of *Dictyocha messanensis*, while Ojin Guyot (DSDP Site 430) yielded a well-preserved and abundant modern mid-latitude silicoflagellate assemblage (Ling, 1980b). In deep-sea cores drilled on Guyot Koko (DSDP

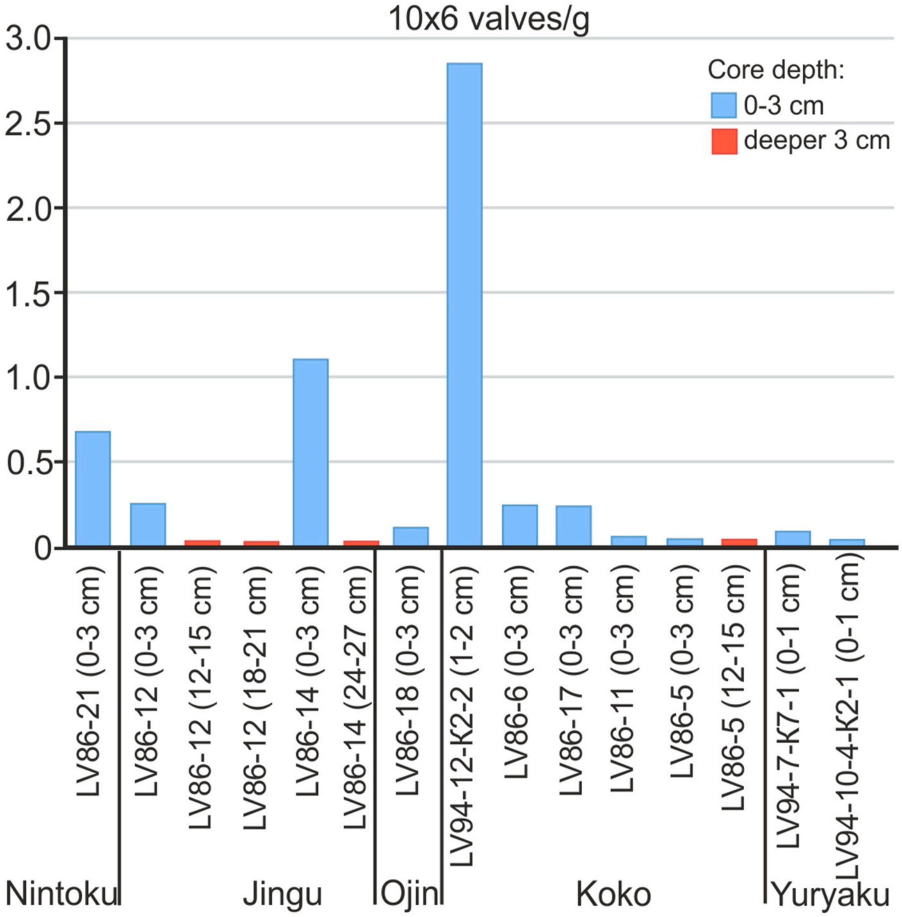

Fig. 10. Concentration of diatoms (mln valves per gram) in sediments of the ESC guyots.

Sites 308, 309), no silicoflagellates were found (Bukry, 1975).

4. Discussion

The radiolarian fauna in the sediments of the ESC southern guyots was represented by taxa characteristic of the transition zone from the arctic-boreal to the tropics, and the content was different. Relatively high numbers of radiolarians were observed in the silty foraminiferal oozes of the lower bathyal zone (1161–2242 m) of the Nintoku, Jingu, Ojin, and Koko guyots. A reduced number of radiolarians was noted in the sediments of the Yuryaku Guyot, which are represented by foraminiferal sands. This distribution of radiolarian concentrations is due to differential preservation of radiolarians and active hydrodynamics. The higher content of radiolarians in silty foraminiferal ooze may be due to the ability of fine particles to protect biogenic silica from dissolution (Zhang et al., 2015).

The content of arctic-boreal species of radiolarians decreases from 45 to 49% on the Nintoku and Jingu guyots to 21–30% on the Koko and Yuryaku guyots. Significant changes in the taxonomic composition of radiolarian assemblages from north to south were noted on the Ojin Guyot. In the sediments of this guyot, a sharp decrease in the number of arctic-boreal species (up to 33%) and an increase in the number of subtropical and tropical species (64%) was noted, compared with the assemblages of the Nintoku and Jingu guyots. The radiolarian assemblage of the Ojin Guyot contains species that are not found north of the Kuroshio Bifurcation Front (Motoyama and Nishimura, 2005). Thus, it can be deduced that the northern boundary of warm waters in the ESC region is located between the Jingu and Ojin guyots. This boundary is also indicated by sharp species differences in the radiolarian assemblages of these guyots. Kamikuri et al. (2008) identified northern and southern subtropical radiolarian assemblages in the subtropical climatic zone, separated by a Subtropical Front. The differences in the radiolarian assemblages also allow us to establish the northern (Nintoku--Jingu guyots) and southern (Ojin-Koko-Yuryaku guyots) radiolarian assemblages in the transitional climatic zone separated by the Kuroshio Bifurcation Current. The distribution boundary of the tropical radiolarian assemblage in the North Pacific in the west runs about 37° N, then in the central part it rises to 44° N and in the east it drops to 30° N (Kruglikova, 1981, 2013). This is explained by the variations of the hydrological regime, since the North Pacific Current has a large influence.

In the sediments of the Koko Guyot, the species *Amphimelissa setosa*, which migrated to the Arctic 0.085–0.04 Ma (Kamikuri et al., 2004; Matul, 2009; Ikenoue et al., 2016; Matsuzaki and Suzuki, 2018) were found, as well as species that are considered Neogene and were not previously found in modern sediments (*Ellipsoxiphus atractus*, *Larcopyle labyrinthusa*, *Stylodictya concentrica*, *Eucyrtidium hexacola*, *Eucyrtidium punktatum*). These species also live in the modern ocean, since the preservation of the skeletons does not show signs of reworking. Since we do not know the ages of the sediments, we cannot establish this with certainty. Neogene deposits were established in the Shatsky Rise (Bralower et al., 2002; Matsuzaki et al., 2023). These deposits may be the source of Neogene radiolarians to the ESC area. The active hydrodynamic regime, especially at 1000–2500 m (Chen et al., 2021), may have contributed to erosion, reworking, and transport of older sediments.

The sediments of the Jingu and Koko guyots contain the species *Cycladophora davisiana*, an indicator of the North Pacific intermediate water (NPIW) (Okazaki et al., 2003, 2004; Hays and Morley, 2003; Itaki and Ikehara, 2004; Matul, 2009). According to Matsuzaki et al. (2020) in

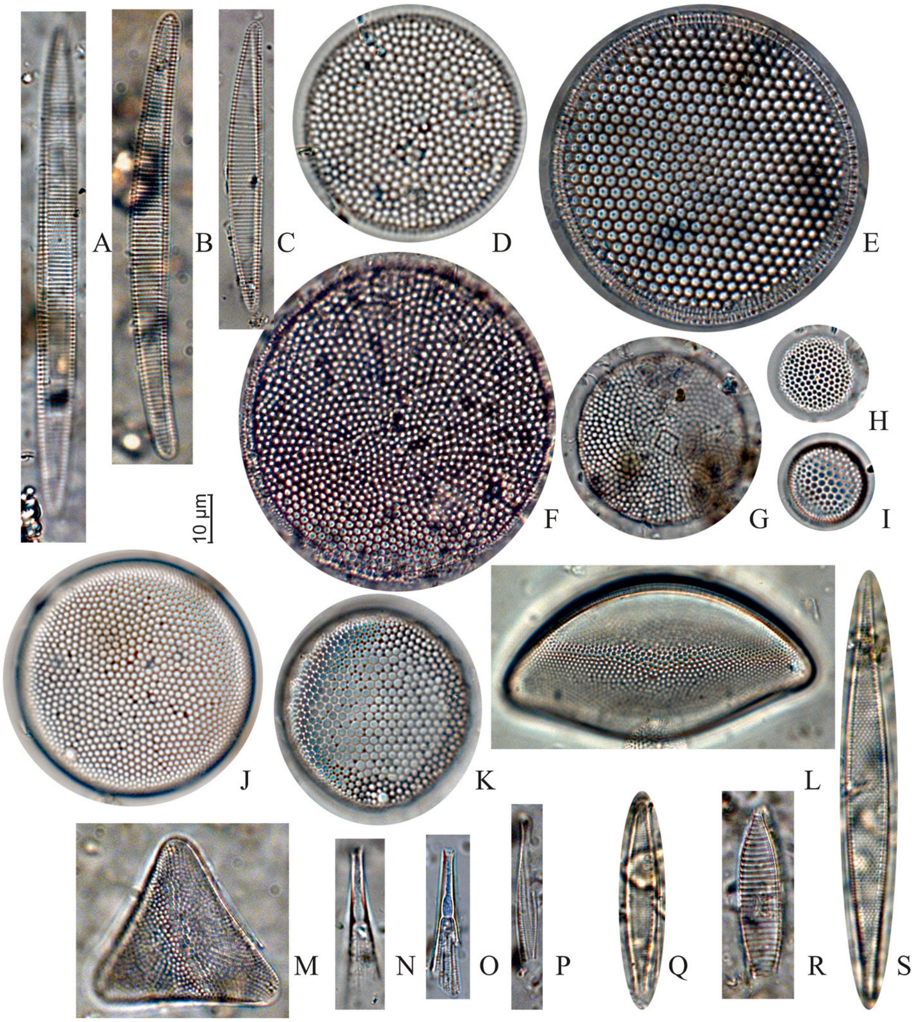

Fig. 11. Tropical and subtropical diatoms from surface sediments of the ESC guyots. **A** – *Alveus marinus* (Grunow) Kaczmarska & Fryxell, sample LV86-17 (0–3 cm). **B, C** – *Fragilariopsis doliolus* (Wallich) Medlin & P.A.Sims, **B** – sample LV86-12 (0–3 cm), **C** – sample LV86-11 (0–3 cm). **D** – *Azpeitia nodulifera* (A.W.F.Schmidt) G.A. Fryxell & P.A.Sims, sample – LV86-21 (0–3 cm). **E** – *Thalassiosira leptopus* (Grunow) Hasle & G.Fryxell, sample LV86-18 (0–3 cm). **F** – *Azpeitia africana* (Janisch ex A. W.F.Schmidt) G.Fryxell & T.P.Watkins, sample LV94-12-K2-2 (1–2 cm). **G** – *Azpeitia tabularis* (Grunow) G.Fryxell & P.A.Sims, sample LV86-11 (0–3 cm). **H, I** – *Shionodiscus oestrupii* (Ostenfeld) A.J.Alverson, S.-H.Kang & E.C.Theriot, sample LV21 (0–3 cm). **J** – *Roperia tesselata* (Roper) Grunow ex Pelletan, sample – LV86-21 (0–3 cm). **K** – *Roperia tesselata* f. *ovata* (Mann) Voigt, sample LV86-12 (0–3 cm). **L** – *Actinocyclus cuneiformis* (Wallich) F.Gómez, Lu Wang & Senjie Lin, sample LV86-21 (0–3 cm). **M** – *Cestodiscus cinnamomeus* (Greville) Grunow, sample LV86-18 (0–3 cm). **N, O** – *Rhizosolenia bergonii* H.Peragallo, **N** – sample LV86-14 (0–3 cm), **O** – sample LV94-7-K7-1 (0–1 cm). **P, Q** – *Nitzschia bicapitata* Cleve, **P** – sample LV94-12-K2-2 (1–2 cm), **Q** – sample LV86-5 (0–3 cm). **R** – *Nitzschia silicula* Hustedt, sample LV94-12-K2-2 (1–2 cm). **S** – *Nitzschia kolaczeckii* Grunow, sample LV86-21 (0–3 cm). Scale bar = 10 µm.

subtropical areas *C. davisiana* inhabits depths below 1000 m and dominates the radiolarian assemblage between 2000 and 3000 m, where the temperature is 3–4 °C. In addition, indicators of NPIW also include *Larcopyle weddellium* and *Pseudodictyophimus gracilipes*, which inhabit depths between 500–1000 and 2000–3000 m in the subtropical Northwest Pacific (Matsuzaki et al., 2020; Matsuzaki, 2023). These species are also present in radiolarian assemblages in sediments collected at bathyal depths (Table S1).

In surface sediments of the North Pacific Ocean, the content of diatoms is considered to be low (5–50 mln valves per gram) (Jousé et al., 1969), which reflects the relatively low productivity in the surface waters of this region (Semina, 1974; Tsoy and Wong, 1999), but in the ESC their content drops almost 8 times (to 1.9 mln valves per gram) (Jousé et al., 1969). The concentrations of diatoms in the surface sediments of the ESC (from 0.1 to 2.83 mln valves per gram) are consistent with these data.

Noticeable amounts of *Paralia sulcata*, isolated finds of species *Actinocyclus octonarius*, *A. octonarius* var. *tenellus*, *A. divisus*, *Actinoptychus senarius*, and *Cyclotella striata*, more typical for coastal areas, as well as benthic brackish water species *Diploneis weissflogii* and the freshwater species *Pinnularia borealis*, raises questions about their source. Some of these species were found in the Quaternary sediments of the Ojin Guyot and in the Neogene sediments of the Suiko Guyot, located north of the Nintoku Guyot (Koizumi, 1980), but *Paralia sulcata* and freshwater species were not found there. One explanation for the appearance of coastal species in the sediments of guyots is their transport by currents (both surface and deep) and with aeolian dust. The top region of most of the guyot sections studied was characterized by active bottom hydrodynamics (Dautova et al., 2019). A study of the composition and geochemistry of the surface sediments of the ESC showed that the hydrodynamic conditions there are much stronger than on the abyssal plain, especially at 1000–2500 m (Chen et al., 2021). Sediments of zone I (33–44°N), which includes the Nintoku, Jingu, and Ojin guyots, contain a significant amount of terrigenous and aeolian material (ibid.), which came from the surrounding land with currents and wind, despite significant distances from the continent.

The Nintoku-Jingu diatom assemblages are characterized by a significant number of boreal elements (11.5–33%) and have a mixed flora,

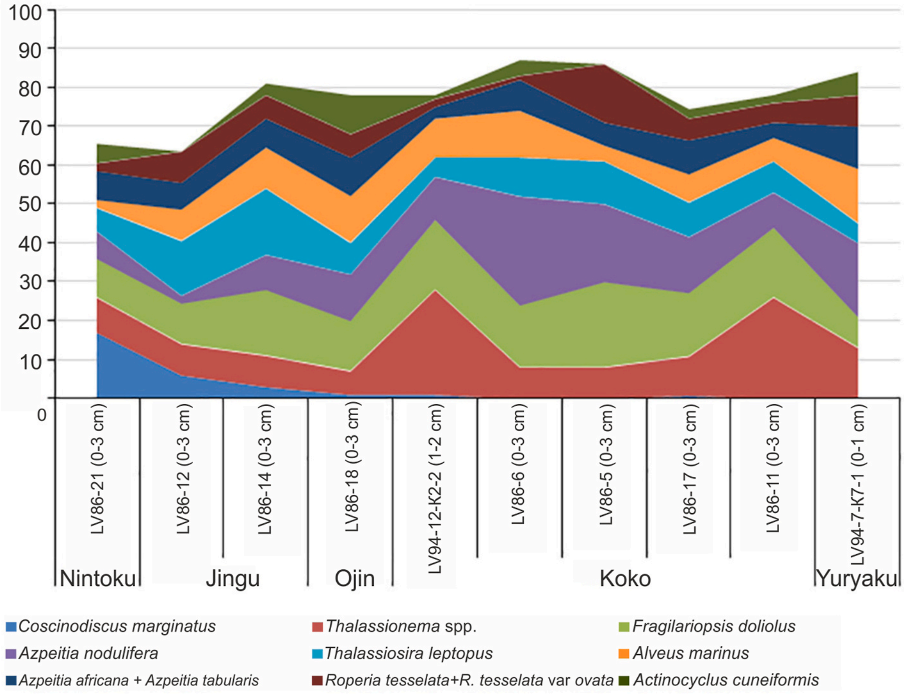

Fig. 12. Percentage of predominant taxa in diatom assemblages in surface sediments of the ESC guoyts.

characteristic of the transition zone between the arctic-boreal and tropical regions (Semina, 1974). The boundaries of phytogeographical regions for phytoplankton are in good agreement with the boundaries in the surface layer of sediments (ibid.). The Ojin-Koko-Yuryaku diatom assemblages consist almost entirely of tropical and subtropical species (68–86%) with a mixture of cosmopolitan species (6–25%). In the Pleistocene-Holocene sediments of the Nintoku Guyot, the diatom assemblage was assigned to the North Pacific *Denticulopsis seminae* Zone, while the diatom assemblage from the sediments of the Ojin Guyot was assigned to the tropical diatom *Pseudoeunotia doliolus* Zone (Koizumi, 1980), which indicates significant differences in diatom assemblages during this period. Differences in diatom and silicoflagellate assemblages from the sediments also suggest that the northern boundary of warm water transported by the Subtropical Gyre between the Ojin and Jingu guyots. Differences in the diatom and silicoflagellate assemblages of the Nintoku-Jingu and Ojin-Koko-Yuryaku guyots probably reflect the influence of the Subarctic factor on the first and warm waters of the Kuroshio Bifurcation Current, the northern boundary of which passes between the Ojin and Jingu guyots.

According to Semina (1974), the northern boundary of the phytogeographical tropical region in sediments is close to that in plankton and passes about 30° N. Our data indicate the difference in the assemblages of diatoms and silicoflagellates at 38° N, but are not sufficient to confirm the position of this boundary, but suggest its migration to the north over the past 50 years due to significant warming of the latter decades in the Northern Hemisphere (IPCC, 2021). Since the early 20th century, and certainly since the 1950s, global mean sea surface temperatures have increased (Bindoff et al., 2007; Hoegh-Guldberg et al., 2014). In the Pacific Ocean, average surface temperatures increased by 0.31 °C (Hoegh-Guldberg et al., 2014) and are associated with the Kuroshio Extension and North Pacific Current (Bindoff et al., 2007).

At approximately the same latitude (between 37 and 39° N) there is a biogeographical boundary established by corals and coinciding with the biogeographical boundary between the boreal and Western Pacific biogeographical regions by the bathyal fauna of brittle stars (*Ophiura*) (Sirenko and Smirnov, 1989; Galkin et al., 2020). This boundary coincides with the Kuroshio Bifurcation Current (Zhang and Hanawa, 1993; Sainz-Trapaga et al., 2001; Motoyama and Nishimura, 2005) which in the ESC flows at 38° N between the Ojin and Jingu guyots.

5. Conclusions

In the sediments (silty foraminiferal oozes and sands) of the Nintoku, Jingu, Ojin, Koko, and Yuryaku guyots of the ESC, a rich fauna of radiolarians and flora of diatoms and silicoflagellates were found. Radiolarians are abundant in the lower bathyal zone (1161–2242 m) of all studied guyots except Yuryaku Guyot, and are rare in the sediments of the upper bathyal zone (777 m) of the Koko Guyot. From 18 to 27 cm they are nearly absent. The concentration of diatoms and silicoflagellates in surface sediments is uneven, and below 0–3 cm decreases sharply. The decrease is probably due to the dissolution of siliceous microfossils and the action of bottom currents. The occurrence of extinct and relatively shallow-water neritic species is likely the result of reworking caused by active hydrodynamics on the ESC guyots and transport by currents. Radiolarians are represented by subtropical and tropical, as well as arctic-boreal species, and the content of the latter sharply decreases towards the south. Diatoms in surface sediments are diverse and abundant and are represented mainly by tropical and subtropical oceanic species, but in the sediments of the Nintoku and Jingu guyots, there is a Subarctic influence. Differences in the radiolarian, diatom and silicoflagellate assemblages of the Nintoku-Jingu and Ojin-Koko-Yuryaku guyots reflect the influence of the Subarctic waters and warm waters of the Kuroshio Bifurcation Current. In the transitional zone, the Kuroshio Bifurcation Current represents a biogeographic boundary separating cold-water and warm-water biota. North of this latitude, sediments on the Jingu and Nintoku guyots are characterized by a mixed radiolarian fauna and diatom flora with a high content of arctic-boreal species. To the south there are species that live only within the subtropical and tropical climatic zones. Thus, two biogeographic assemblages are identified, separated by the Kuroshio Biffurcation Current. The Nintoku-Jingu assemblage consists of approximately equal numbers of arctic-boreal and subtropical species, and the Ojin-Koko-Yuryaku assemblage consists of predominantly subtropical and tropical species with a minor content of arctic-boreal species.

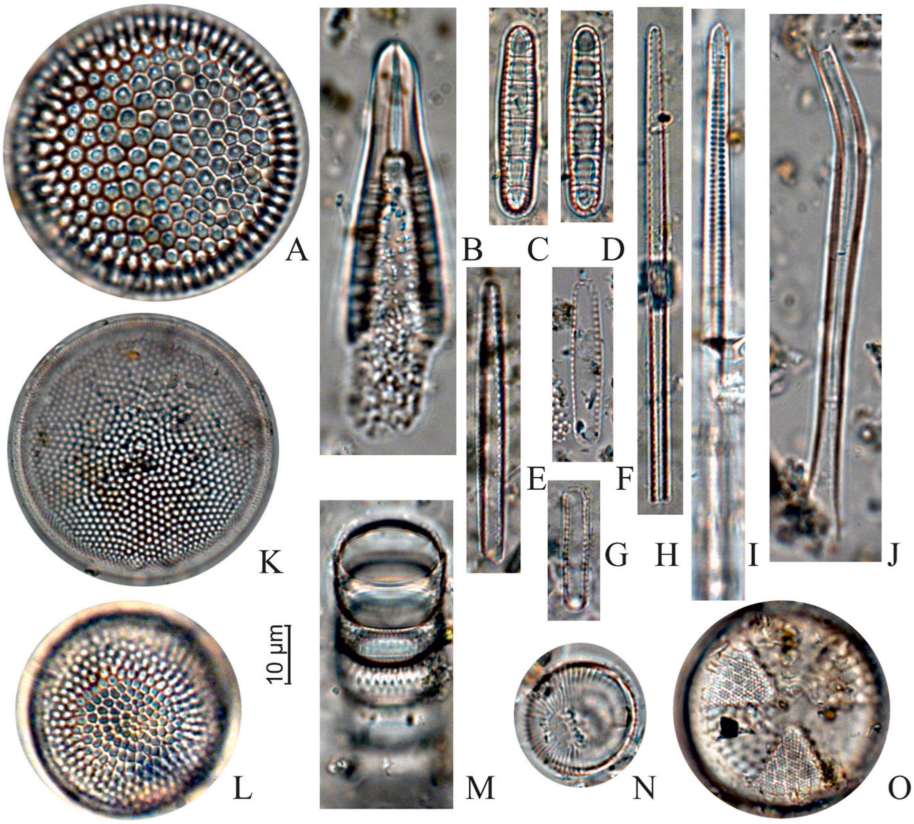

Fig. 13. Arctic-boreal, boreal, and cosmopolitan diatoms from surface sediments of the ESC guyots. **A –** *Coscinodiscus marginatus* Ehrenberg, sample LV86-21 (0–3 cm). **B** – *Rhizosolenia hebetata* Bailey, sample LV86-21 (0–3 cm). **C, D** – *Neodenticula seminae* (Simonsen & T.Kanaya) Akiba & Yanagisawa, **C** – sample LV86-11 (0–3 cm), **D** – sample Lv86-5 (0–3 cm). **E, F** – *Thalassionema nitzschioides* (Grunow) Mereschkowsky, **E** – sample LV94-12-K2-2 (1–2 cm), **F** – sample LV86-14 (0–3 cm). **G** – *Thalassionema nitzschioides* var. *parvum* Heiden & Kolbe, sample LV94-12 K2-2 (1–2 cm). **H** – *Thalassionema frauenfeldii* (Grunow) Tempère & Peragallo, sample LV94-7 K7-1 (0–1 cm). **I** – *Thalassiothrix longissima* Cleve & Grunow, sample LV86-21 (0–3 cm). **J** – *Proboscia subarctica* K.Takahashi, R.W.Jordan & J.Priddle, sample LV86-14 (0–3 cm). **K** – *Actinocyclus curvatulus* Janisch, sample LV86-14 (0–3 cm). **L** – *Thalassiosira antarctica* Comber (resting spore), sample LV86-21 (0–3 cm). **M** – *Paralia sulcata* (Ehrenberg) Cleve, sample LV86-12 (0–3 cm). **N** – *Cyclotella striata* (Kützing) Grunow, sample LV86-12 (0–3 cm). **O** – *Actinoptychus senarius* (Ehrenberg) Ehrenberg, sample LV86-14 (0–3 cm). Scale bar = 10 µm.

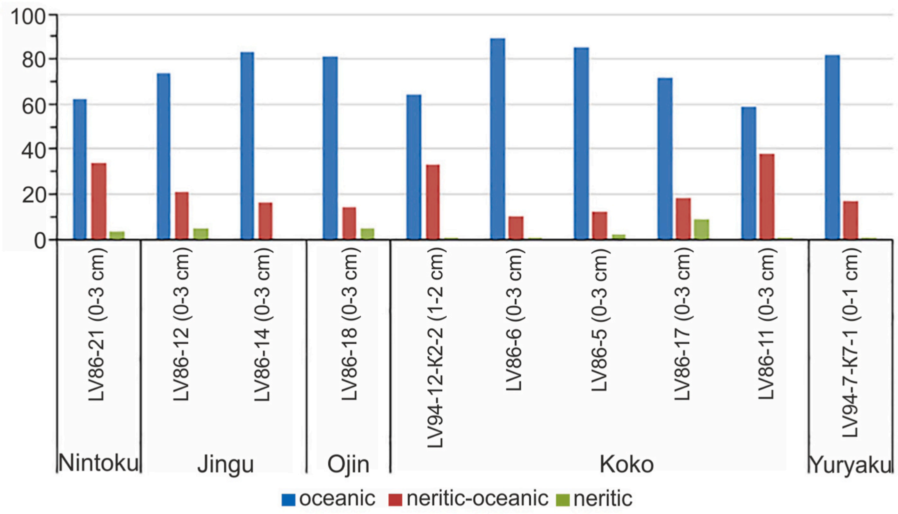

Fig. 14. Percentage of oceanic, neritic-oceanic (panthalassic), and neritic diatoms in diatom assemblages from surface sediments of the ESC guyots.

CRediT authorship contribution statement

Lidiya N. Vasilenko: Writing – original draft, Methodology, Investigation, Conceptualization. **Ira B. Tsoy:** Writing – original draft, Methodology, Investigation, Conceptualization. **Tatyana N. Dautova:** Writing – original draft, Methodology, Investigation, Conceptualization.

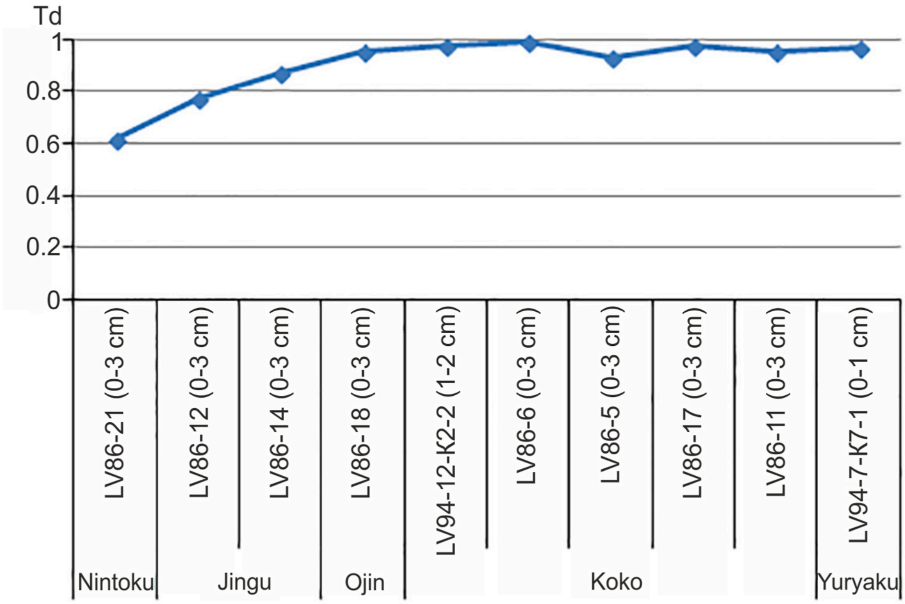

Fig. 15. Changes in the diatom temperature index (Td) in surface sediments of the ESC guyots (from north to south).

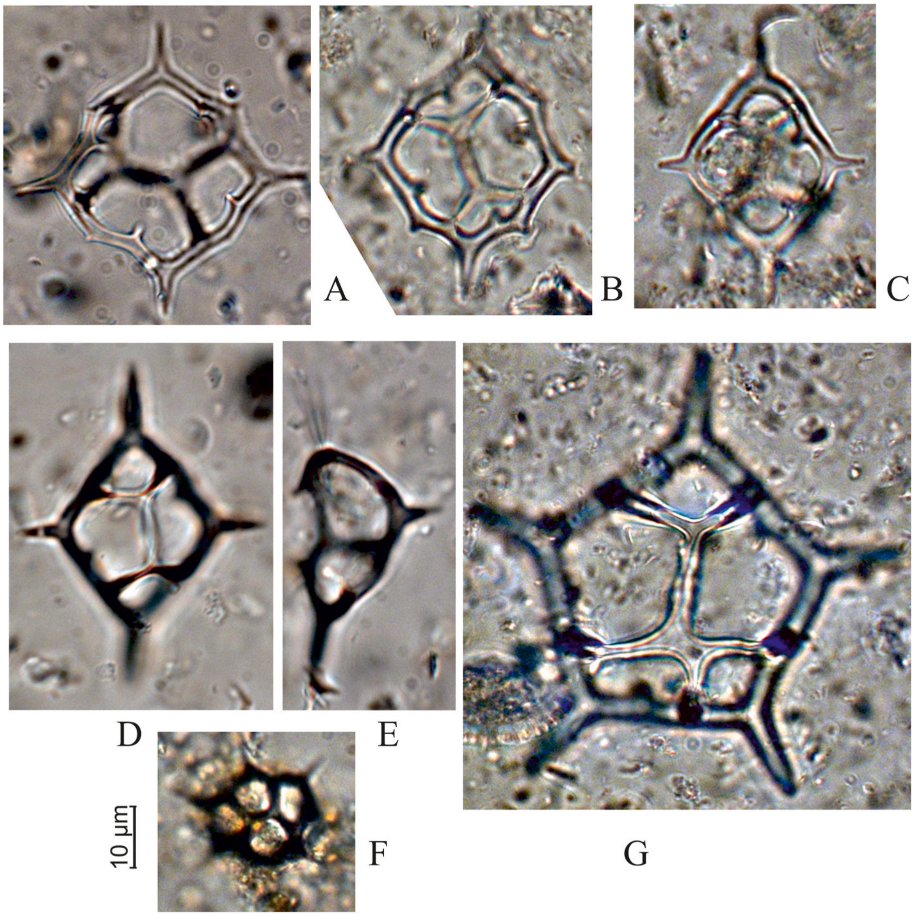

Fig. 16. Silicoflagellates from surface sediments of the ESC guyots. **A, B** – *Dictyocha epiodon* Ehrenberg, **A** – sample LV86–21 (0–3 cm), **B** – sample LV94-12-K2-2 (1–2 cm). **C** – *Dictyocha fibul*a Ehrenberg, sample LV94-12-K2-2 (1–2 cm). **D, E** – *Dictyocha messanensis* Haeckel, sample LV86-21 (0–3 cm). **F** – *Octactis speculum* (Ehrenberg) F.H.Chang, J.M.Grieve & J.E.Sutherland, sample LV86-18 (0–3 cm). **G** – *Dictyocha pentagona* (P.Schulz) Bukry & J.H.Foster, sample LV94-12-K2-2 (1–2 cm). **F** – *Octactis speculum* (Ehrenberg) F.H.Chang, J.M.Grieve & J.E.Sutherland, sample LV86-12 (0–3 cm). Scale bar = 10 μm.

Funding

This study was funded by the Ministry of Sciences and Education of the Russian Federation (project number 124022100084-8).

Declaration of competing interest

The authors declare that they have no known competing financial interests or personal relationships that could have appeared to influence the work reported in this paper.

Acknowledgments

We are grateful to A.V. Zhirmunsky National Scientific Center of Marine Biology, Far Eastern Branch of Russian Academy of Sciences for samples obtained during the Cruises 86 and 94 of the *RV Akademik M.A. Lavrentyev*. We thank the captain and crew of the *RV Akademik M.A. Lavrentyev* and the team of the ROV Comanche 18 for collecting bottom sediments. We are grateful to Lidiya Osipova for processing samples for microscopic study of diatoms and silicoflagellates and Daria Khmel for processing samples for microscopic study of radiolarians. Special thanks to Vyacheslav Lobanov for valuable comments on the hydrology of the Northwest Pacific Ocean. We also thank the anonymous reviewers and Editor-in-Chief Walker O. Smith for their comments and suggestions for improving the article.

Appendix A. Supplementary data

Supplementary data to this article can be found online at https://doi.org/10.1016/j.dsr2.2024.105433.

Data availability

No data was used for the research described in the article.

References

Afanasieva, M.S., Amon, E.O., 2006. Radiolarians. PIN RAS, Moscow.

Bailey, J.W., 1856. Notice of microscopic forms found in the soundings of the Sea of Kamtschatka. Am. J. Sci. Arts, Second series 22 (64), 1–6.

Barron, J.A., 2003. Planktonic marine diatom record of the past 18 m.y.: appearance and extinctions in the Pacific and Southern oceans. Diatom Res. 18 (2), 203–224.

Belyaeva, T.V., 1963. Composition and distribution of diatoms in the surface layer of Pacific Ocean sediments. Oceanology 3 (4), 684–695.

Bernstein, R.L., White, W.B., 1981. Stationary and traveling mesoscale perturbationsin the Kuroshio extension current. J. Phys. Oceanogr. 11, 692–704.

Bindoff, N.L., Willebrand, J., Artale, V., Cazenave, A., Gregory, J., Guley, S., Hanawa, K., Le Quere, C., Levitus, S., Nojiri, Y., Shum, C.K., Talley, L.D., Unnikrishnan, A., 2007. Observations: oceanic climate change and sea level. In: Climate Change 2007: the Physical Science Basis. Contribution of Working Group I to the Fourth Assessment Report of the. Intergovernmental Panel on Climate Change Cambridge University Press, Cambridge, United Kingdom and New York, NY, USA, pp. 387–429.

Boltovskoy, D., Correa, N., 2016. Biogeography of radiolaria polycystina (protista) in the world ocean. Prog. Oceanogr. 149, 82–105.

Bralower, T.J., Premoli Silva, I., Malone, M.J., Arthur, M.A., Avery, K., Bown, P.R., et al., 2002. Proceedings of the Ocean Drilling Program initial reports 198. Ocean Drilling Program. https://doi.org/10.2973/odp.proc.ir.198.2002.

Bukry, D., 1975. Coccolith and silicoflagellate stratigraphy, northwestern Pacific Ocean, deep Sea Drilling project Leg 32. In: Initial Reports of the Deep Sea Drilling Project, vol. 32. U.S. Govt. Print. Office, Washington, pp. 677–701, 32.

Bukry, D., Foster, J.H., 1973. Silicoflagellate and diatom stratigraphy, Leg 16, deep Sea Drilling project. In: Init. Repts. DSDP, 16, vol. 16. U.S. Govt. Print. Office, Washington, pp. 815–871.

Chang, F.H., Sutherland, J., Bradford-Grieve, J., 2017. Taxonomic revision of Dictyochales (Dictyochophyceae) based on morphological, ultrastructural, biochemicaland molecular data. Phycol. Res. 65, 235–247. https://doi.org/10.1111/pre.12181.

Chen, C., Wang, C., Li, H., Hu, D., Li, G., Chen, X., He, Y., 2023. Detection and characteristics analysis of the western subarctic front using the high-resolution SST product. Acta Oceanol. Sin. 42, 24–32. https://doi.org/10.1007/s13131-022-2102-5.

Chen, J., Zou, J., Zhu, A., Shi, X., Nürnberg, D., Lembke-Jene, L., Tiedemann, R., Wang, K., Wu, Y., Dong, Z., Liu, J., Dou, R., 2021. Geochemistry of surface sediments from the emperor seamount chain, North Pacific. Front. Earth Sci. 9, 674842. https://doi.org/10.3389/feart.2021.674842.

Clague, D.A., Dalrymple, G.B., Moberly, R., 1975. Petrography and K-Ar ages of dredged volcanic rocks from the western Hawaiian Ridge and southern Emperor Seamount Chain. Geol. Soc. Am. Bull. 86, 991–998.

Clague, D.A., Dalrymple, G.B., 1973. Age of Koko seamount, emperor. Seamount chain. Earth Planet Sci. Lett. 17, 411–415.

Clague, D.A., Dalrymple, G.B., 1987. The Hawaiian-Emperor volcanic Chain. Part I. Geologic evolution 1, 5–54. USGS professional paper 1350.

Dalrymple, G.B., Garcia, M.O., 1980. Age and chemistry of volcanic rocks dredged from Jingu Seamount, Emperor seamount chain, Init. Rep. of the Deep Sea Drilling Project 55, 685–693.

Dautova, T.N., Galkin, S.V., Tabachnik, K.R., 2019. The first data on the structure of vulnerable marine ecosystems of the emperor chain seamounts: indicator taxa, landscapes, and biogeography. Russ. J. Mar. Biol. 45 (6), 408–417. https://doi.org/10.1134/S1063074019060026.

Davies, T.A., Wilde, P., Clague, D.A., 1972. Koko seamount: a major guyot at the southern end of the Emperor seamounts. Mar. Geol. 13 (5), 311–321. https://doi.org/10.1016/0025-3227(72)90013-8.

Desikachary, T.V., Prema, P., 1996. Silicoflagellates (Dictyochophyceae), vol. 100. J. Cramer, Berlin; Stuttgart (Ser. Bibliotheca Phycologica. V.

Dodimead, A.G., Favorite, A.E., Hirano, T., 1963. Salmon of the North Pacific Ocean, Part II, review of oceanography of the subarctic pacific region. Bull. Int. North Pac. Fish. Comm. 13, 1–195.

Dutkiewicz, A., Callaghan, S.O., Muller, R.D., 2016. Controls on the distribution of deep-sea sediments. G-cubed 17, 3075–3098. https://doi.org/10.1002/2016GC006428.

Ermakov, YuG., Ignatiev, G.M., Kurakova, L.I., et al., 1988. Physical Geography of Continents and Oceans. Higher school, Moscow.

Galkin, S.V., Dautova, T.N., Minin, K.V., Tabachnik, K.R., 2020. Biological investigations of emperor seamount chain using a remotely operated vehicle Comanche. Oceanology 60 (2), 293–294. https://doi.org/10.1134/S0001437020010117.

Garcia, N., Odebrecht, C., 2012. Remarks on the morphology and distribution of some rare centric diatoms in Southern Brazilian continental shelf and slope waters. Braz. J. Oceanogr. 60 (4), 415–442. https://doi.org/10.1590/S1679-87592012000400002.

Haeckel, E., 1862. Die Radiolarien (Rhizopoda Radiata). Berlin.

Haeckel, E., 1887. Report on the radiolaria collected by the H.M.S. «Glomar challenger» during the years 1873-1876. Rep. sci. results of the vojage of H.M.S. Challenger during the years 1873-1876 //Zoology. Edinburg, 18. Pt. 1, 2.

Harrison, K.G., 2000. Role of increased marine silica input on paleo-pCO2 levels. Paleoceanography 15, 292–298. https://doi.org/10.1029/1999PA000427.

Hasle, G.R., Syversten, E.E., 1997. Marine diatoms. Identifying Marine Phytoplankton. Academic press, London.

Hays, J.D., 1970. Stratigraphy and evolutionary trends of radiolaria in North Pacific deep-sea sediments. Geological investigations of the North pacific. Geol. Soc. Am. Mem. 126, 185–218.

Hays, J.D., Morley, J.J., 2003. The Sea of okhotsk: a window on the ice age ocean. Deep-Sea Res. I 50, 1481–1506.

Hernandez-Becerril, D.U., Bravo-Sierra, E., 2001. Planktonic silicoflagellates (dictyochophyceae) from the Mexican Pacific Ocean. Bot. Mar. 44, 4172423. https://doi.org/10.1515/BOT.2001.050.

Hoegh-Guldberg, O., Cai, R., Poloczanska, E.S., et al., 2014. The Ocean. In: Climate Change 2014: Impacts, Adaptation, and Vulnerability. Part B: Regional Aspects. Contribution of Working Group II to the Fifth Assessment Report of the Intergovernmental Panel on Climate. Cambridge University Press, Cambridge, United Kingdom and New York, NY, USA, pp. 1655–1731.

Ikenoue, T., Okazaki, Y., Takahashi, K., Sakamoto, T., 2016. Bering Sea radiolarian biostratigraphy and paleoceanography at IODP Site U1341 during the last four million years. Deep Sea Res. II 125–126, 38–55. https://doi.org/10.1016/j.dsr2.2015.03.004.

IPCC (The Intergovernmental Panel on Climate Change), 2021. Climate Change 2021: the Physical Science Basis. Cambridge University Press, Cambridge. https://doi.org/10.1017/9781009157896.

Ishitani, Y., Takahashi, K., 2007. The vertical distribution of Radiolaria in the waters surrounding Japan. Mar. Micropaleontol. 65, 113–136.

Itaki, T., Ikehara, K., 2004. Middle to late Holocene changes of the Okhotsk Sea Intermediate Water and their relation to atmospheric circulation. Geophys. Res. Lett. 31, L24309. https://doi.org/10.1029/2004GL021384.

Itoh, S., Yasuda, I., 2010. Characteristics of mesoscale eddies in the kuroshio-oyashio extension region detected from the distribution of the sea surface height anomaly. J. Phys. Oceanogr. 40, 1018–1034. https://doi.org/10.1175/2009JPO42265.1.

Jackson, E.D., Koizumi, I., Dalrymple, G.B., Clague, D.A., Kirkpatrick, R.J., 1980. Introduction and summary of results from DSDP Leg 55, the Hawaiian-emperor hot-spot experiment. Init. Rep. DSDP 55, 5–31.

Jordan, R.W., McCartney, K., 2015. *Stephanocha* nom. nov., a replacement name for the illegitimate silicoflagellate genus *Distephanus* (Dictyochophyceae). Phytotaxa 201 (3), 177–187. https://doi.org/10.11646/phytotaxa.201.3.1.

Jousé, A.P., 1977. Atlas of Microorganisms in Bottom Sediments of the Oceans (Diatoms, Radiolarians, Silicoflagellates, Coccoliths). Nauka, Moscow.

Jousé, A.P., Kazarina, G.H., 1974. Pleistocene diatoms from site 262, Leg 27, DSDP. In: Inittial Reports of the Deep Sea Drilling Project, vol. 27. U.S. Govt. Print. Office, Washington, pp. 925–945.

Jousé, A.P., Mukhina, V.V., Kozlova, O.G., 1969. Distribution of diatoms in the surface layer of sediments from the Pacific Ocean. In: The Pacific Ocean. Microflora and Microfauna in the Recent Sediments of the Pacific. Nauka, Moscow, pp. 7–47.

Jousé, A.P., Proshkina-Lavrenko, A.I., Sheshukova-Poretskaya, V.S., 1974. Research methodology. In: Diatom Algae of the USSR. Fossil and Recent, vol. I. Nauka, Moscow, pp. 50–79.

Kaczmarska, I., Fryxell, G.A., 1996. *Alveus*, gen. nov. (Bacillariaceae, Bacillariophyta), a heavily silicified diatom found in warm water oceans. Microsc. Res. Tech. 33, 2–11.

Kamikuri, S., Nishi, H., Motoyama, I., Saito, S., 2004. Middle Miocene to Pleistocene radiolarian biostratigraphy in the Northwest Pacific ocean. Ocean Drilling Program, Leg 186. Isl. Arc 13, 191–226. https://doi.org/10.1111/j.1440-1738.2003.00421.x.

Kamikuri, S., Motoyama, I., Nishimura, A., 2008. Radiolarian assemblages in surface sediments along longitude 175°E in the Pacific Ocean. Mar. Micropaleontol. 69, 151–172. https://doi.org/10.1016/j.marmicro.2008.07.005.

Karpoff, A.-M., 1980. The sedimentary deposits of Suiko seamount (Leg 55, site 433): from the reef environment to the pelagic sedimentation. Init. Rep. DSDP 55, 491–501.

Karpoff, A.-M., Peterschmitt, I., Hoffert, M., 1980. Mineralogy and geochemistry of sedimentary deposits on emperor seamounts, sites 430, 431, and 432: authigenesis of silicates, phosphates, and ferromanganese oxides. Init. Rep. DSDP 55, 461–489.

Kawai, H., 1972. Hydrography of the Kuroshio extension. In: Yoshida, H. Stommeland K. (Ed.), Kuroshio, its Physical Aspects. Univ. of Tokyo Press, Tokyo, pp. 235–352.

Kazarina, G.K., Yushina, I.G., 1999. Diatoms in recent and holocene sediments of the north pacific and the bering sea. Ber. Polarforsch. 306, 134–148.

Kling, S., Boltovskoy, D., 1995. Radiolarian vertical distribution patterns across the southern California Current. Deep-Sea Res. I 42, 191–231.

Koizumi, I., 1980. Neogene diatoms from the emperor seamount chain, Leg 55 deep Sea Drilling project. In: Initial Reports of the Deep Sea Drilling Project, vol. 55. U.S. Govt. Print. Office, Washington, pp. 387–407. https://doi.org/10.13140/RG.2.1.1480.9681, 55.

Koizumi, I., 1986. Late Neogene temperature record in the Northwest Pacific ocean. Sci. Rep. Coll. Gen. Educ. Osaka Univ. 34, 145–153.

Koizumi, I., Butt, A., Ling, H.Y., Takayama, T., 1980. Biostratigraphic summary of DSDP Leg 55: emperor seamount chain. Init. Rep. DSDP 55, 285–288.

Konovalova, G.V., Orlova, T.Y., Pautova, L.A., 1989. Atlas of Phytoplankton of the Sea of Japan. Nauka, Leningrad.

Kozyrenko, T.F., Strelnikova, N.I., Khursevich, G.K., Tsoy, I.B., Jakovschikova, T.K., Muchina, V.V., Olshtynskaja, A.P., Semina, G.I., 2008. The Diatoms of Russia and Adjacent Countries. Fossil and Recent, vol. II. St.-Petersburg University Press, St.-Petersburg issue 5.

Kruglikova, S.B., 1981. Some features of the ecology and distribution of modern and Cenozoic radiolarians. Systematics, Evolution and Stratigraphic Significance of Radiolarians. Nauka, Moskow, pp. 118–139.

Kruglikova, S.B., 2013. Radiolarians-Polycystina from the Bottom Sediments of the World Ocean as Bioindicators of Environmental Fluctuations. GEOS. Moskow.

Lazarus, D., Faust, K., Popova-Goll, I., 2005. New species of prunoid radiolarians from the Antarctic Neogene. J. Micropalaeontol. 24 (2), 97–121.

Ling, H.Y., 1980a. Radiolarians from the emperor seamounts of the Northwest Pacific, Leg 55 of the deep Sea Drilling project. In: Jackson, E.D., Koizumi, I., et al. (Eds.), Init. Repts. DSDP, vol. 55. U.S. Govt. Printing Office, Washington, pp. 365–373, 55.

Ling, H.Yi, 1980b. Silicoflagellates and ebridians from Leg 55. In: Initial Reports of the Deep Sea Drilling Project, vol. 55. U.S. Govt. Print. Office, Washington, pp. 375–385, 55.

Lipman, R.K., 1979. Guide to the Study of Fossil Radiolarians. Nedra, Moscow.

Lisitsyn, A.P., 1974. Sedimentation in the Oceans. Publishing House Nauka, Moscow.

Lisitsyn, A.P., 1978. Processes of Ocean Sedimentation. Publishing House Nauka, Moscow.

Lombari, G., Boden, G., 1985. Modern Radiolarian Global Distribution. Cushman Foundation for Foraminiferal Research Special Publication, pp. 1–125.

Makarova, I.V., Strelnikova, N.I., Kozyrenko, T.F., et al., 2002. The Diatoms of Russia and Adjacent Countries. Fossil and Recent, vol. II. St.-Petersburg University Press, St.-Petersburg issue 2.

Matsuzaki, K.M., 2023. Evolution of oceanography of the central Northwest Pacific over the past 10 million years with focus on late Miocene global cooling. Paleoceanogr. Paleoclimatol. 38, e2023PA004789. https://doi.org/10.1029/2023PA004789.

Matsuzaki, K.M., Itaki, T., 2017. New northwest Pacific radiolarian data as a tool to estimate past sea surface and intermediate water temperatures. Paleoceanography 32, 218–245. https://doi.org/10.1002/2017PA003087.

Matsuzaki, K.M., Itaki, T., Sugisaki, S., 2020. Polycystine radiolarians vertical distribution in the subtropical Northwest Pacific during Spring 2015 (KS15-4). Paleontol. Res. 24 (2), 113–133. https://doi.org/10.2517/2019PR019.

Matsuzaki, K.M., Suzuki, N., 2018. Quaternary radiolarian biostratigraphy in the subarctic northeastern Pacific (IODP Expedition 341 Site U1417) and synchroneity of bioevents across the North Pacific. J. Micropalaeontol. 37, 1–10. https://doi.org/10.5194/jm-37-1-2018.

Matul, A.G., 2009. Quaternary Biostratigraphy and Paleoceanology of the Sea of Okhotsk and Other Subarctic Areas. GEOS, Moscow.

Mizuno, K., White, W.B., 1983. Annual and interannual variability in the Kuroshio current system. J. Phys. Oceanogr. 13, 1847–1867.

Motoyama, I., Nishimura, A., 2005. Distribution of radiolarians in North Pacific surface sediments along the 175°E meridian. Paleontol. Res. 9 (2), 95–117.

Nelson, D.M., Tréguer, P., Brzezinski, M.A., Leynaert, A., Quéguiner, B., 1995. Production and dissolution of biogenic silica in the ocean: revised global estimates, comparison with regional data and relationship to biogenic sedimentation. Global Biochem. Cycle. 9 (3), 359–372. https://doi.org/10.1029/95GB01070.

Nigrini, C., 1970. Radiolarian assemblages in the North pacific and their application to a study of quaternary sediments in core V20-130. In: Hays, J.D. (Ed.), Geological Investigations of the North Pacific, vol. 126. Geological Society of America. Memoir, pp. 139–183. https://doi.org/10.1130/MEM126-p139.

Okazaki, Y., Takahashi, K., Itaki, T., Kawasaki, Y., 2004. Comparison of radiolarian vertical distributions in the okhotsk sea near the kuril islands and in the north-western North Pacific off hokkaido island. Mar. Micropaleontol. 51, 257–284. https://doi.org/10.1016/j.marmicro.2004.01.003.

Okazaki, Y., Takahashi, K., Onodera, J., Honda, M.C., 2005. Temporal and spatial flux changes of radiolarians in the northwestern Pacific Ocean during 1997–2000. Deep Sea Res. Part II Top. Stud. Oceanogr. 52 (16–18), 2240–2274. https://doi.org/10.1016/j.dsr2.2005.07.006.

Okazaki, Y., Takahashi, K., Yoshitani, H., Nakatsuka, T., Ikehara, M., Wakatsuchi, M., 2003. Radiolarians under the seasonally sea-ice covered conditions in the Okhotsk Sea: flux and their implications for paleoceanography. Mar. Micropaleontol. 49, 195–230. https://doi.org/10.1016/S0377-8398(03)00037-9.

Poelchau, H.S., 1976. Distribution of holocene silicoflagellates inNorth pacific sediments. Micropaleontology 22 (2), 164–193.

Pushkar, C.S., Cherepanova, M.V., 2001. Diatoms of Pliocene and Antropogene of the North Pacific. Dalnauka, Vladivostok.

Ren, J., Gersonde, R., Esper, O., Sancetta, C., 2014. Diatom distributions in northern North Pacific surface sediments and their relationship to modern environmental variables. Palaeogeogr. Palaeoclimatol. Palaeoecol. 402, 81–103. https://doi.org/10.1016/j.palaeo.2014.03.008.

Renz, G.W., 1976. The Distribution and Ecology of Radiolaria in the Central Pacific: Plankton and Surface Sediments, vol. 22. Bulletin of the Scripps Institution of Oceanography, University of California, San Diego.

Reshetnyak, V.V., 1966. The deep-water radiolarian Phaeodaria in the northwestem part of the Pacific Ocean. In: Fauna of the USSR, Radiolaria. Akad. Nauk. USSR, Zool. Inst., N. Ser., vol. 94. Nauka, Moscow-Leningrad.

Roden, G.I., Taft, B.A., Ebbesmeyer, C.C., 1982. Oceanographic aspects of the emperor seamounts region. J. Geophys. Res. 87, 9537–9552.

Romero, O.E., Armand, L.K., Crosta, X., Pichon, J.-J., 2005. The biogeography of major diatom taxa in Southern Ocean surface sediments: 3. Tropical/Subtropical species. Palaeogeogr. Palaeoclimatol. Palaeoecol. 223, 49–65. https://doi.org/10.1016/J.palaeo.2005.03.027.

Round, F.E., Crawford, R.M., Mann, D.G., 1990. The Diatoms: Biology and Morphology of the Genera. Cambridge University Press, Cambridge.

Sainz-Trapaga, S.M., Goni, G.J., Sugimoto, T., 2001. Identification of the Kuroshio Extension, its bifurcation and northern branch from altimetry and hydrographic data during October 1992–August 1999: spatial and temporal variability. Geophys. Res. Lett. 28 (9), 1759–1762. https://doi.org/10.1029/2000GL012323.

Saito, K., Ozima, M., 1977. 40Ar-39Ar geochronological studies on submarine rocks. Earth Planet Sci. Lett. 33, 353–369.

Sancetta, C., Silvestri, S., 1986. Pliocene–Pleistocene evolution of the North Pacific Ocean–atmosphere system, interpreted from fossil diatoms. Paleoceanography 1, 163–180.

Semina, H.J., 1974. Pacific Phytoplankton. Nauka, Moscow.

Sirenko, B.I., Smirnov, I.S., 1989. Refinement of the biogeographic boundary in the North pacific thalassobathial based on the benthic fauna of the imperial mountains. Geography of the world ocean. Abstracts of the Report of the IV All-Russian Conference on the Geography of the World Ocean. House of the USSR Academy of Sciences, pp. 124–125.

Takahashi, K., 1987. Seasonal fluxes of silicoflagellates and *Actiniscus* in the subarctic Pacific during 1982-1984. J. Mar. Res. 45, 397–425.

Takahashi, K., 1991. Radiolaria: flux, ecology, and taxonomy in the Pacific and Atlantic. In: Honjo, S. (Ed.), Ocean Biocoenosis. Woods Hole Oceanographic Institution Press, USA. Series 3.

Tanimura, Y., Shimada, C., Iwai, M., 2007. Modern distribution of *Thalassionema* species (bacillariophyceae) in the Pacific Ocean. Bull National Mus Nat Sci. 33, 27–51.

Tarduno, J.A., Duncan, R.A., Scholl, D.W., et al., 2002. Leg 197 summary. In: Proc. ODP, Init. Repts., vol. 197. College Station, TX (Ocean Drilling Program), pp. 1–92.

Tochilina, S.V., 1985. Biostratigraphy of the Cenozoic of the Northwestern Pacific. Nauka, Moscow.

Tochilina, S.V., 1996. On the Problem of the Systematics of Nassellaria (Radiolaria). Biochemical peculiarities. Evolution. FEB RAS, Vladivostok.

Tochilina, S.V., Vasilenko, L.N., 2018. Atlas of Cenozoic Radiolarians from the Northwest Pacific. POI FEB RAS, Vladivostok.

Tréguer, P., Bowler, C., Moriceau, B., Dutkiewicz, S., Gehlen, M., Aumont, O., et al., 2018. Influence of diatom diversity on the ocean biological carbon pump. Nat. Geosci. 11 (1), 27–37. https://doi.org/10.1038/s41561-017-0028-x.

Tsoy, I.B., Obrezkova, M.S., Artemova, A.V., 2009. Diatoms in surface sediments of the sea of okhotsk and the Northwest Pacific ocean. Oceanology 49 (1), 130–139. https://doi.org/10.1134/S0001437009010159.

Tsoy, I.B., Shastina, V.V., 1999. Neogene Siliceous Microplankton of the Japan Sea (Diatoms and Radiolarians). Dalnauka, Vladivostok. https://doi.org/10.13140/RG.2.1.2788.9364.

Tsoy, I.B., Wong, C.S., 1999. Diatom fluxes and preservation in the deep north west pacific. In: 14th International Diatom Symposium, Tokyo, Sept. 2-8, 1996. Proceedings of the 14th Intern. Diatom Symposium. Koeltz Scien. Books, Koenigstein, Germany, pp. 523–549.

Vasilenko, L.N., Vasilenko, YuP., 2021. Pleistocene radiolarian biostratigraphy of the submarine vityaz ridge, Northwest Pacific. Mar. Micropaleontol. 169, 102040. https://doi.org/10.1016/j.marmicro.2021.102040.

Vasiliev, B.I., 2009. The Geological Structure and Origin of the Pacific Ocean. Dal'nauka, Vladivostok.

Volokhin, YuG., Melnikov, M.E., Shkolnik, E.L., 1995. Guoyts of the Western Pacific and Their Mineralization. Nauka, Moscow.

Wang, R., Biskaborn, B.K., Ramisch, A., Ren, J., Zhang, Y., Gersonde, R., 2016. Modern modes of provenance and dispersal of terrigenous sediments in the North Pacific and Bering Sea: implications and perspectives for palaeoenvironmental reconstructions. Geo Mar. Lett. 36, 259–270. https://doi.org/10.1007/s00367-016-0445-7.

Wong, C.S., Whitney, F., Tsoy, I.B., Bychkov, A.S., 1995. The opal pump and subarctic carbon removal. In: global fluxes of carbon and its related substances in the coastal sea-ocean-atmosphere system. In: Tsunogai, S., et al. (Eds.), Proceedings of the 1994 Sapporo IGBP Symposium. M & J International, Yokohama, Japan, pp. 339–344.

Yamashita, H., Takahashi, K., Fujitani, N., 2002. Zonal and vertical distribution of radiolarians in the western and central Equatorial Pacific in January 1999. Deep-Sea Research II 49, 2823–2862. https://doi.org/10.1016/S0967-0645(02)00060-7.

Yamauchi, M., 1986. The distribution of radiolarian assemblages in surface sediments from the northwestern Pacific. News of Osaka Micropaleontologists, Special 7, 141–156.

Yuan, X., Talley, D., 1996. The subarctic frontal zone in the North Pacific: characteristics of frontal structure from climatological data and synoptic surveys. J. Geophys. Res. 101 (C7), 16491–16508.

Zhang, R., Hanawa, K., 1993. Features of the water-mass front in the northwestern North Pacific. J. Geophys. Res. 98, 967–975.

Zhang, L., Wang, R., Chen, M., et al., 2015. Biogenic silica in surface sediments of the south China Sea: controlling factors and paleoenvironmental implications. Deep Sea Res. Part II: topical Stud. Oceanogr. 122, 142–152. https://doi.org/10.1016/j.dsr2.2015.11.008.

Zhang, L., Suzuki, N., Nakamura, Y., Tuji, A., 2018. Modern shallow water radiolarians with photosynthetic microbiota in the western North Pacific. Mar. Micropaleontol. 139, 1–27. https://doi.org/10.1016/j.marmicro.2017.10.007.

Further readings

Benson, R.N., 1966. Recent Radiolaria from the Gulf of California University of Minnesota Ph.D. thesis.

Boltovskoy, D., 1987. Sedimentary record of radiolarian biogeography in the equatorial to Antarctic Micropaleontology. western Pacific Ocean 33, 267–281.

Lazarus, D., Suzuki, N., Caulet, J.P., Nigrini, C., Goll, I., Goll, R., Dolven, J.K., Diver, P., Sanfilippo, A., 2015. An evaluated list of Cenozoic-Recent radiolarian species names (Polycyctinea), based on those used in the DSDP, ODP and IODP deep-sea drilling programs. Zootaxa 3999 (3), 301–333. https://doi.org/10.11646/zootaxa.3999.3.1.

Muchina, V.V., 1969. Biostratigraphy of sediments and questions of paleogeography of the tropical region of the Pacific and Indian oceans. In: Micropaleontology and Organogenous Sedimentation in the Oceans. Nauka, Moscow, pp. 84–95.

O'Dogherty, L., Caulet, J.-P., Dumitrica, P., Suzuki, N., 2021. Catalogue of cenozoic radiolarian genera (class polycystinea). Geodiversitas 43 (21), 709–1185. https://doi.org/10.5252/geodiversitas2021v43a21. http://geodiversitas.com/43/21.

Trubovitz, S., Renaudie, J., Lazarus, D., Noble, P., 2022. Late Neogene lophophaenidae (Nassellaria, radiolaria) from the eastern equatorial pacific. Zootaxa 5160 (1), 1–158. https://doi.org/10.11646/zootaxa.5160.1.1.

Tsoy, I.B., 2011. Silicoflagellates of the oligocene–early Miocene submarine vityaz ridge (island slope of the kurile–kamchatka trench). Al Gologiya 1, 111–125.

Vasilenko, L.N., Khmel, D.S., 2024. New Radiolarian Species of the Genus Carpocanium Ehrenberg, 1847, emend. nov. in the Surface Sediments of the Emperor Seamount Chain. Pacific Ocean. Paleontol. J. 58 (6), 619–629. https://doi.org/10.1134/S0031030124600938.